NOTE TO USERS

COMBINED PHOTOCATALYTIC AND ELECTROCHEMICAL TREATMENT OF ORGANIC MATTER AND HEAVY METALS

BY

COLIN LAM

B. ENG (RYERSON)

A Thesis Project

Presented to Ryerson University

In partial fulfillment of the Requirements for the degree of

Master of Engineering

In

Chemical Engineering

Toronto, Ontario, Canada, 2004

Toronto, Ontario, Canada, 2004

Author's Declaration

I hereby declare that I am the sole author of this report.

I authorize Ryerson University to lend this report to other institutions or individuals for the purpose of scholarly research.

Colin Lam

I further authorize Ryerson Polytechnic University to reproduce this report by photocopying or by other means, in total or parts, at the request of other institutions or individuals for the scholarly research.

Colin Lam

Ryerson University requires the signature of all persons using or photocopying this thesis. Please sign below, and give address and date.

NAME	ADDRESS	DATE

Acknowledgements

The author wishes to thank his family and friends who have been incredibly supportive throughout his years at Ryerson Polytechnic University and to Dr. Doan for his assistance in the completion of this paper. The author also wishes to express his thanks to Mr. Ali. Hemmati, and Mr. P. Scharping for providing support in the laboratory.

Abstract

Combined Photocatalytic and Electrochemical treatment of organic matter and heavy metals, Colin Lam, Ryerson University, 2004, Master of Engineering in Chemical Engineering.

In the present study, simulated wastewater containing Methylene Blue, Zn^{2+} and Ni^{2+} was treated by two treatment methods: photocatalytic oxidation and electrochemical deposition. It is found that Methylene Blue could be degraded more efficiently by combined Photocatlytic and Electrochemical process than by photocatalytic oxidation or electrochemical deposition alone. The percentage removal of Methylene Blue in combined Suspended Photocatalytic and Electrochemical process was 46.1% after 72 hours of treatment, while it was only 36.1% for a single Suspended Photocatalytic process and 23.5% for a single Electrochemical process. On the other hand, no significant effect were observed for the percentage removal of Zn^{2+} and Ni^{2+} in combined Suspended Photocatalytic and Electrochemical process. The influence of liquid flowrate, wavelength and pH to the removal of Methylene Blue, Zn^{2+} and Ni^{2+} was also investigated.

Table of contents

List of Figures

List of Tables

Nomenclature

[AS]	concentration of occupied sites (mol/L)
[S]	concentration of free sites (mol/L)
A_e	Electrode Area (m^2)
c	speed of the light (2.998 x 10^8m/s in vacuum)
C	concentration (mol/L)
c_i	Initial concentration (mol/m^3)
E	Specific energy (kJ)
E_h	potential (V)
$E_{h,n}$	Ground potential or Standard potential (V)
E_g	Band Gap energy (eV)
F	Faraday's constant = 96500 (coulombs)
h	Planck's constant (6.63 x 10^{-34}Js)
I	current (A)
i	current density (I/A_e)
K	ka/kd is the adsorption constant / apparent adsorption constant
k	the rate constant
k'	kK (1/s)
k_a	the rate of constant of adsorption (1/s)
k_d	the rate of constant of desorption (1/s)
m	mass of metal ion concentration at time t
m_o	mass of metal ion concentration at time 0
P	partial pressure of A (Pa)
R	Gas constant = 8.31 m^3.Pa/mol.K
r_a	rate of adsorption (mol/s)
r_d	rate of desorption (mol/s)

T	Temperature (^{o}C)
t	time (sec/min/h)
v	frequency of the radiation (Hz)
v_e	stoichiometric coefficient of electrons
θ	The coverage
λ	wavelength (nm)

CHAPTER 1 – INTRODUCTION AND OBJECTIVES

1.1 Introduction

Most of the industrial operations discharge some wastewater that goes into the environment. As the wastewater is hazardous to human and natural living things, wastewater treatments are necessary. Water treatment is described as the removal of contaminants in wastewater or a water body. In practice, a wastewater treatment facility typically sets the goal to manage the waste stream to a higher quality and harmless to the receiving body given that the economic cost is reasonable (Metcalf & Eddy, 2003). Wastewater treatment process usually combines physical, chemical and biological methods. Wastewater treatment plants are classified as primary, secondary, or tertiary (advanced) treatment, depending on the purification level to which the plants treat (Drinan, 2001). However, as current and pending wastewater regulations require lower concentrations of pollutants in industrial wastewater, advanced wastewater treatment is required to remove the pollutants that remain after conventional treatment technology. One such example is industrial wastewater containing both organic and inorganic (heavy metal) pollutants. There are very strict legislative requirements that govern the treatment and disposal of such waste, mainly due to the potential of severe environmental consequences in the event of non-compliance.

Advanced wastewater treatment is defined as the additional treatment needed to remove suspended, colloidal, and dissolved constituents remaining after the conventional secondary treatment. Dissolved constituents may vary from relatively simple inorganic ions, such as calcium, potassium, sulfate, nitrate and phosphate, to an ever increasing number of highly complex synthetic organic compounds. In order to meet the increasing

stringent wastewater treatment requirements in terms of both limiting concentration of many of these substances in the treatment plant effluent and establishing effluent toxicity limits, advanced wastewater treatment is required to remove the pollutants which remain after conventional treatment technology.

The need for advanced wastewater treatment is based on consideration of the following factors:

1. The need to remove organic matter and total suspended solids beyond what can be accomplished by conventional treatment processes to meet stringent discharge requirements.
2. The need to remove residual total suspended solids to condition the treated wastewater for more effective disinfection.
3. The need to remove nutrients beyond what can be accomplished by conventional secondary treatment process to limit eutrophication of sensitive water bodies.
4. The need to remove specific inorganic (e.g. heavy metals, silica) and organic constituents for industrial reuse, surface water disposal and for indirect potable reuse applications (eg., ground water recharge) (Metcalf & Eddy, 2003).

This project was investigation of the removal of the organic and heavy metals in wastewater using photocatalytic and electrochemical treatment simultaneously.

1.2 Objectives

The objectives of the present study were:

- To investigate the individual and combined Electrochemical and Photocatalytic treatment of model organics and heavy metals with suspended titanium dioxide.
- To investigate the behaviour of the Photocatalytic treatment of Methylene Blue
- To investigate the effect of various process parameters on the pollutant removal including:

1. Liquid Flowrate
2. Wavelength of the ultraviolet light
3. pH of the wastewater

- To test the immobilization of TiO_2 in the Rotating Photocatalytic Reactor
- To investigate the combined Electrochemical and Photocatalytic treatment of model organics and heavy metals with immobilized titanium dioxide

CHAPTER 2 – LITERATURE SURVEY

2.1 Advanced Oxidation processes

Chemical oxidation may not oxidize a given compound or group of compounds completely. In many cases, partial oxidation is sufficient to render specific compounds more amenable to subsequent biological treatment or to reduce their toxicity. Advanced Oxidation Processes (AOPs) are used to oxidize complex organic matters found in wastewater, which are difficult to degrade biologically into simpler end products. The oxidation of specific compounds may be characterized as follows:

1. Primary Degradation: A structural change in the parent compound
2. Acceptable degradation: A structural change in the parent compound to the extent the toxicity is reduced.
3. Ultimate degradation (Mineralization): Conversion of organic carbon to inorganic CO_2.
4. Unacceptable degradation: A structural change in the parent compound resulting in increased toxicity.

Advanced Oxidation Processes typically involve the generation and use of the hydroxyl free radical (HO•) as a strong oxidant to destroy compounds that cannot be oxidized by conventional oxidants such as oxygen, ozone, and chlorine. The hydroxyl radical is one of the most active oxidants known. The hydroxyl radical reacts with the dissolved pollutants, initiating a series of oxidation reactions until the constituents are completely mineralized. Due to their nonselective reaction with pollutants and their ability to operate at normal temperature and pressures, hydroxyl radicals are capable of oxidizing almost all reduced materials present in wastewater without restriction to specific classes or

groups of compounds, as compared to other oxidants. One of the major differences between advanced oxidation and other treatment processes (such as ion exchange or stripping) is that the pollutants in wastewater are degraded rather than concentrated or transferred into a different phase. Since secondary waste materials are not generated, there is no need to dispose of or regenerate materials (Metcalf & Eddy, 2003).

Among various Advanced Oxidation Processes, (AOPs), the heterogeneous photocatalytic process with titanium dioxide for the destruction of pollutants in water and air, has been the subject of much research recently (Dionysiou et al, 2000). Through years of research by various researchers, heterogeneous photocatalysis was found as an emerging destructive technology leading to the total mineralization of most of organic pollutants (Guillard et al, 2003). In the present study, heterogenous photocatalytic process was proposed to degrade organic matter in the wastewater.

2.2 Electrochemical Deposition

Industrial wastewater, which contains inorganic pollutants much as heavy metals, is not easy to treat as metal ions are generally non-degradable. They have infinite lifetimes and build up their concentrations in food chains to toxic levels. In recent years, numerous methods of the treatment for metals increase significantly with the development of industry. Thus, waste metal recovery can potentially resolve two issues: metals pollution prevention and simultaneously resource conservation. Precipitation, activated carbon adsorption, ion exchange, and membrane separations are common methods currently adopted for the treatment of metal ions in wastewater (Pelizzetti and Serpone, 1989). All these methods have their own advantages and disadvantages. One of the emerging technologies that can potentially resolve the two issues is the electrochemical deposition of metal ions by electrochemical method. The electrochemical treatment of metal ion pollutants has several advantages as compared to the ones stated above, including the following:

1. The metal is normally produced in its most valuable form, which is the metallic form, and may be reused or recycled.
2. No extra reagents are added, and so the treated water or solution can often be recycled.
3. Sludge production is minimized.
4. The corresponding anodic reaction can be advantageously used; for example, undesirable complexing agents such as cyanide and various chelating agents and other organics may be destroyed at the anode of the same cell (Rajeshwar and Ibanez, 1997).

2.3 Fundamental engineering aspects of Heterogeneous Photocatalytic reactors for water and wastewater treatment

The effectiveness of the Heterogeneous Photocatalytic process is strongly dependent on the reactor design. The utilization of radiation and solid catalysts in a synergic effect for performing chemical transformations of species present in liquid mixtures makes the heterogeneous photocatalytic process more complex than other systems. For example, when stirred dispersions are used, the presence of suspended solid particles makes fluid dynamic complications. The opacity, light scattering and depth of radiation penetrations are also important factors affecting the efficiency of the process. In general, the main difficulties in the heterogeneous photocatalytic reactors are:

1. The fluid dynamics of a fluid solid system is highly non-ideal so that modeling of the specific system is generally needed.
2. The kinetics of a heterogeneous photocatalytic reaction is affected in a complex way by the concentration and the radiation fields that are influenced by the fluid dynamics. The set of conservation equations that model the photoreactor can only be solved numerically.

These challenges slowed down the application of research findings on the photocatalytic oxidation of pollutants in wastewater to commercial processes.

In addition, the difficulty of the commercialization of the photocatlytic oxidation method using suspended catalyst in water and wastewater treatment stems basically from the fact that the post-treatment removal of the semi-conductor catalyst causes a significant off-set in the benefits that might have been derived from the photocatalytic mineralization process. The photocatalyst particle size typically falls in a range between

30–300 mm. Therefore, the removal of materials of these minute diameters necessitates the use of costly phase separation processes. Several alternatives have been proposed for dealing with the problem of the post-treatment removal of the photocatalyst. The approach has generally been to anchor the semi-conductor photocatalyst particles onto supports that are more readily removable (Skelton and Fabiyi, 2000).

2.4 Heterogeneous Photoreactors

The design of the heterogeneous photoreactors is vital to the performance of the organic degradation process. Over the past decades, many types of reactors have been developed. In this section, some of the common photoreactors will be described (Schizvello, 1997):

1. Immersion well photoreactors
2. Annular reactors
3. Film type photoreactors
4. Rotating photoreactors

1. Immersion well photoreactors

This is the simplest type of photoreactor, typically used in a laboratory scale as well as in a pilot scale. It is basically a stirred tank reactor in which solid titanium dioxide particles are generally suspended in liquid. One or more lamps are immersed in the suspension. In many cases conventional reactors are modified by mounting lamps well through their covers.

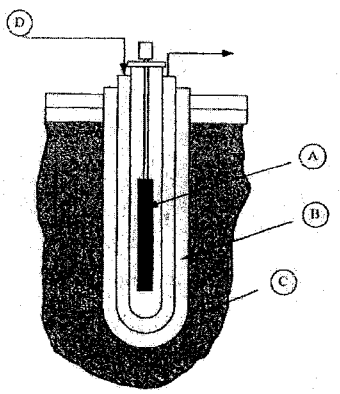

A –Lamp B – Transparent medium C-Wastewater D-Cooling water inlet
Figure 2.1 - Immersion Well Photoreactor (Schiavello, 1997)

It can operate in a batch or continuous way. The main advantage of this type of photoreactor is simplicity and very high photonic efficiency, whereas the disadvantages are:

1. In prolonged use, a thin film of very fine titanium dioxide particles is usually deposited on the lamp surface. Thus, the radiation decreases with time. To avoid this problem the lamp must be cleaned at fixed intervals.
2. Scale-up is unreliable to certain extent depending on the difficulty of modeling the very complex radiation field.

2. Annular Photoreactor

In this kind of reactor the reactive zone is limited by two coaxial cylinders. The lamp is placed on the symmetry axis. It can operate in batch or continuous way. Practically all of the photons emitted by the lamp reach the reacting medium. This type of reactor can utilize immobilized photocatalytic process by immobilizing the titanium dioxide on the outer walls of the reactor.

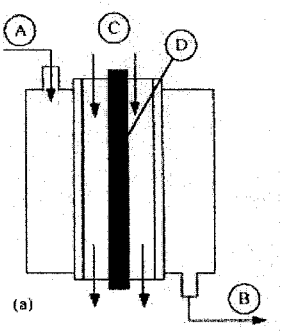

A)Wastewater Inlet B)Wastewater Outlet, C) Cooling medium D) Lamp
Figure 2.2 - Annular Photoreactor (Schiavello, 1997)

3. Film Type Photoreactor

In this kind of photoreactor the reacting mediums forms a thin film of flowing liquid on the reactor wall which is externally irradiated. Usually this type of reactor is used for the evaluation of the immobilized titanium dioxide films. One of the typical reactors is shown in the following figure 2.3.

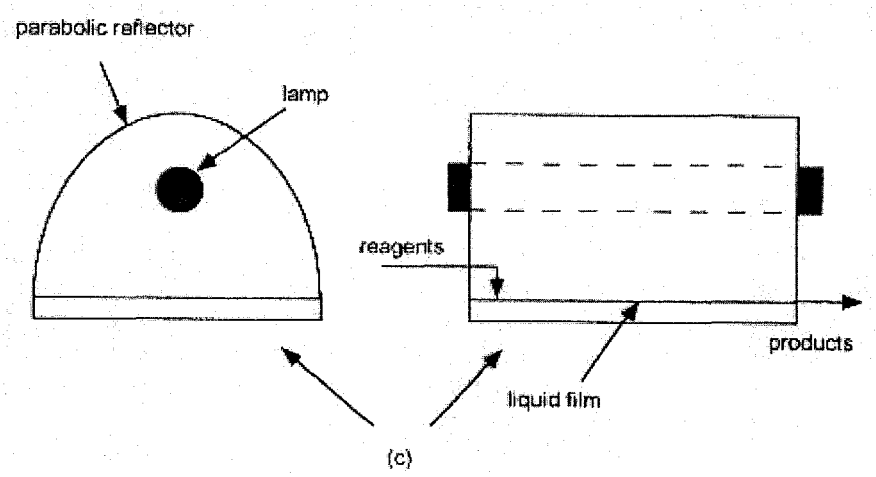

Figure 2.3 - An example of thin film Photoreactor (Schiavello, 1997)

4. Rotating Photoreactor

Rotating photo-reactor makes use of immobilized photocatalyst. The basic design of this type of reactor is shown as the figure below:

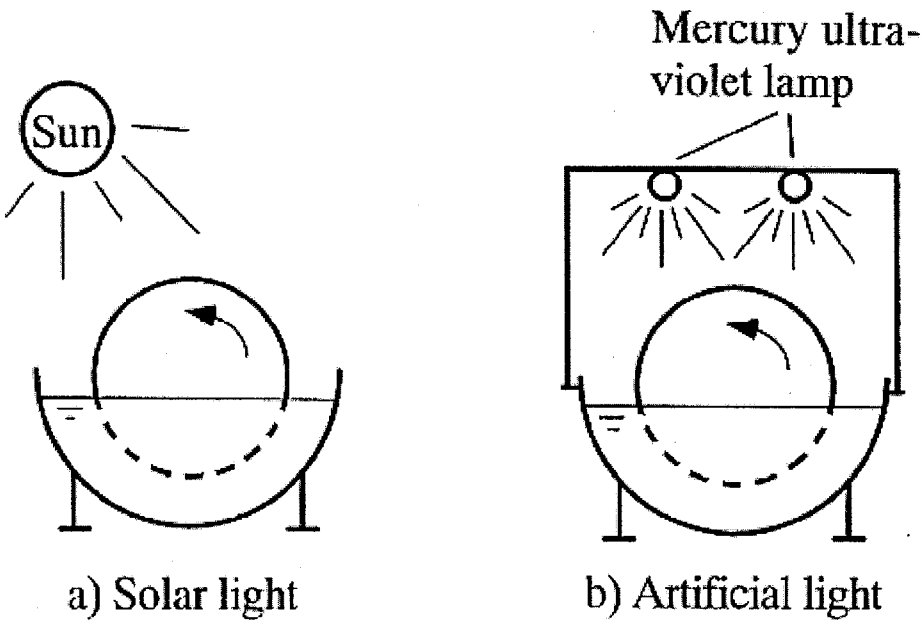

Figure 2.4 – Examples of Rotating Photoreactor (Zheng et al, 2001)

According to Dionysiou et al, the major advantages for this type of reactor include (Dionysiou et al 2000):

1. Immobilization of the titanium dioxide photocatalyst.
2. Reaction within a thin liquid film.
3. Good mixing. The mixing in the rotating photoreactor resembles closely to a ideal CSTR.
4. Ability to replace commercial UV light with natural sunlight, which would reduce the operating cost.
5. No demand for oxygenation other than oxygen uptake from the surrounding air.

In the present study, a Rotating Photoreactor was used to treat a simulated wastewater containing organics and heavy metals.

CHAPTER 3 – LITERATURE BACKGROUND

3.1.1 Heterogeneous Photocatalysis

By definition, photocatalysis can be defined as "acceleration of a photoreaction by the presence of a catalyst" (Pelizzetti and Serpone, 1989). Heterogeneous photocatalytic procress for water and air purification is one of the Advanced Oxidation Processes that have been studied extensively. Heterogenous photocatalytic process can be defined as catalytic process during which one or more reaction steps occur by means of electron-hole pairs photogenerated on the surface of solid semiconductor materials illuminated by lights of suitable energy. Heterogeneous photocatalysis can be carried out in various media: gas phase, pure organic liquid or aqueous phases (Schiavello, 1997). For heterogenous catalysis, the overall process can be decomposed into five major steps (Janssen and Van Satten, 1999):

1. Transfer of the reactants in the fluid phase to the surface of the solid photocatalyst
2. Adsorption of the reactants to the photocatalyst
3. Reaction in the adsorbed phase
4. Desorption of the products from the photocatalyst surface
5. Removal of the products from the solid fluid interface region

In step 3, the photocatalytic reaction occurs in the adsorbed phase. The only difference between the photocatalytic reaction and the catalytic reaction is the mode of activation of the catalyst in which the thermal activation is replaced by a photonic activation at a semiconductor surface. For the photocatalytic reaction the rate increases as a consequence of an optical excitation of a solid that remains chemically unchanged

(Schiavello, 1997). It is evident that steps 1 and 5 of the catalytic process must also occur for the photocatalytic process. Moreover, it must be outlined that the adsorption-desorption processes (step 2 and 4) are also essential in the photocatalytic process and they are also affected by the light irradiation.

A photocatalytic reaction can be described as occurring via the following steps:

a) Photogeneration of electro-hole pairs by exciting a semiconductor with radiation of suitable light energy;

b) Separation of electro-hole pairs by traps that have a trapping rate higher than the recombination rate;

c) Redox reaction by the separated electrons and holes with adsorbed substrates;

d) Evolution of the products and regeneration of the catalytic surface (Schiavello, 1987).

The last step (step d) of the photocatalytic process indeed includes steps 4 and 5. The peculiarity of the photocatalytic process is in step 3 (surface reaction) which develops according to steps a, b and c. Therefore, a photocatalytic process is of the redox type, occurring through the separated holes and electrons, photogenerated by exciting a semiconductor with light. This working mechanism for the photocatalytic process can be defined as "redox mechanism" and the role of the light is mainly to excite the solid which must be a semiconductor (Janssen and Van Santen, 1999).

3.1.2 Nature of light

In order to facilitate a photocatalytic process that can be used to degrade pollutants in water, the role of excitation of the semiconductor by light is important. "Light" is the electromagnetic radiation in the visible, near-ultraviolet, and near-infared spectral range. In the wave model, electromagnetic radiation is characterized by a wavelength, λ, a frequency, ν, and a velocity, c. The three quantities are related by the general equation: (Zumdahl, 1995)

$$\lambda \nu = c \tag{3.1}$$

Wavelength is the distance between two consecutive peaks or troughs in a wave. The frequency is defined as the number of waves per second that pass a given point in space (Zumdahl, 1995). The value of c is the speed of the light (2.998 x 10^8m/s in vacuum), whereas λ and ν assume a wide range of values. The SI values for λ and ν are meters and hertz, respectively. The electromagnetic spectrum encompasses a range of radiation from gamma-rays to radio waves, distinguished by their wavelengths as shown in the figure below.

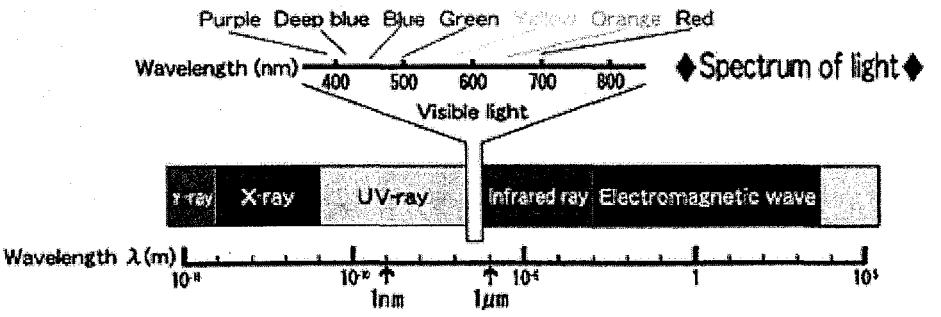

Figure 3.1-The electromagnetic spectrum Source: http://www.arc-flash.co.jp/arc/e/02f.html

In photochemistry we are concerned with the region ranging from 100 to 1000nm. In the quantum model a beam of radiation is regarded as a stream of photons. A photon has no mass but it has a specific energy, E, related to the frequency of the radiation, v, by the Planck relation:

$$E=hv \tag{3.2}$$

Where h is the Planck's constant (6.63×10^{-34}Js). Substiuting equation (3.1), the above equation can be rearranged to:

$$E=\frac{hc}{\lambda} \tag{3.3}$$

The interaction of light with molecular systems is generally an interaction between a molecule and one photon. It can be written in the general form of:

$$A + hv \rightarrow {}^*A \tag{3.4}$$

Where A denotes the ground state molecule, hv the absorbed photon, and *A the molecule in an "excited state". The excited molecule is the molecule A with an extra energy hv. This extra energy and the particular properties, which confer on the molecule, cause the photochemical process (Pelizzetti and Serpone, 1989).

3.1.3 Theory of Semiconductor material and Titanium dioxide as the Photocatalyst

As previously described, the first step of the photocatalytic oxidation process is the photogeneration of electro-hole pairs by exciting a semiconductor with radiation of suitable light energy. Unlike metals, semiconductors are characterized by two separated energy bands: a filled low-energy valance band and an empty high-energy conduction band (Pelizzetti and Serpone, 1989) The energy difference between the filled valance band to the bottom of the vacant conduction band is known as the energy band gap Callister, 1999):

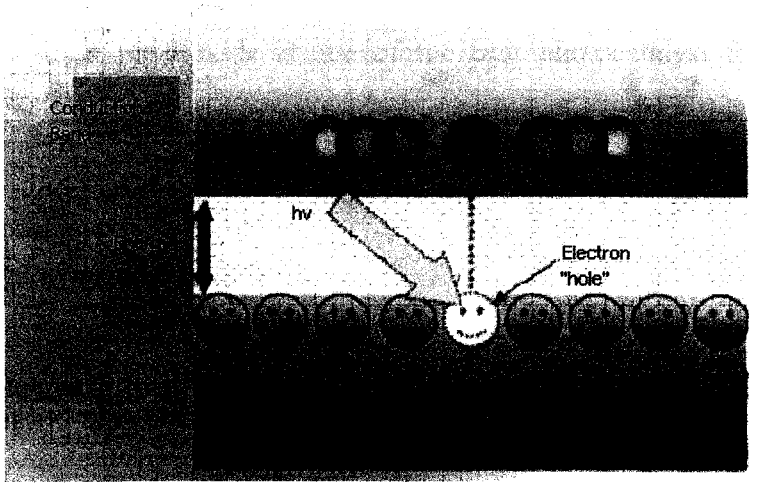

Figure 3.2 - Simplified energy band diagram for a semiconductor (www.ndhu.edu.tw/~k12center/scshool/school6.ppt)

When the semiconductor is irradiated with light energy, the light radiation is absorbed by two basic mechanisms. One of these is electronic polarization which is important only at light frequencies in the vicinity of the relaxation frequency of the constituent atoms. The other mechanism involves valence band-conduction band electron transitions, which depends on the electron energy band structure of the material.

Absorption of a photon of light may cause the excitation of an electron from the nearly filled valance band, across the band gap, and into an empty state within the conduction band, as shown from the figure above (3.2); a free electron in the conduction band and a hole in the valance band are created. The energy of excitation, ΔE, is related to the absorbed photon frequency through equation (3.3) The excitation with the accompanying photoabsorption can take place only if the photon energy is greater than that of the band gap energy, E_g, that is if

$$\frac{hc}{\lambda} > E_g \tag{3.4}$$

In practice, there are many semiconductors that functioned as the photocatalyst. It is well documented that titanium dioxide is one of the best photocatalyst for environmental application. Advantages of titanium dioxide over other semiconductors include:

1. High activity
2. Large stability to light illumination
3. Relatively low cost as compared to other semiconductors
4. Nontoxicity

Based on the equation (3.4), for anatase-type titanium dioxide the band gap energy is 3.2 electron volts (eV), which corresponds to UV light with a wavelength of 388 nanometers (Fujishima et al, 1999).

In summary, light excitation of the semiconductor promotes the electrons from the valance to the conduction band. This UV irradiation generates an electron-hole pair which has an energy equal or greater than the energy band gap of a semiconductor (>3.2

eV for titanium dioxide), generates an electron-hole pair as described in the following equation (Malato and Dibier, 2002):

$$TiO_2 + hv \rightarrow e_{cb}^- + h_{vb}^+ \quad (3.5)$$

3.1.4 Thermodynamics and kinetics of heterogeneous photocatalytic process

From a physical point of view, light absorption by a semiconductor such as titanium dioxide, induces the formation of electron hole pairs. The photo produced pairs can subsequently evolve in different ways (Schiavello, 1997):

1. They can recombine with emission of thermal energy and/or luminescence as shown below (Malato and Dibier, 2002):

$$e_{cb}^- + h_{vb}^+ \rightarrow TiO_2 + \text{energy (heat)} \quad (3.6)$$

2. They can react with electron acceptor or donor species giving rise to reduction and oxidation processes, respectively.

In the area of water and waster treatment, the 2nd pathway, redox reaction with the electron-hole pair leads to the oxidation of aqueous pollutants. The reaction pathways can be summarized by the simple diagram below:

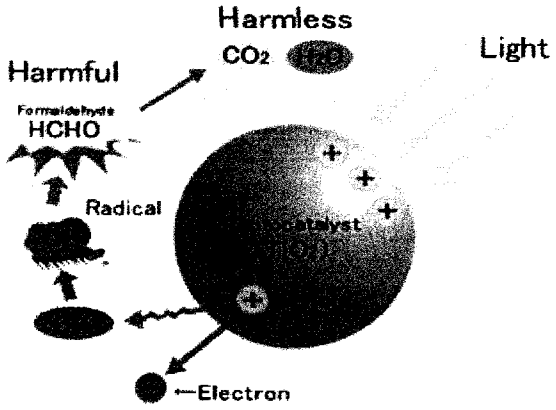

Figure 3.3 – An overall graphical representation of the photocatalytic process with TiO_2 (Source: http://www.arc-flash.co.jp/arc/e/02f.html)

In order to drive the reaction to the 2nd path, oxygen, the most common electron acceptor in aqueous system, would act as the electron scavengers to $O_2^{\bullet -}$ as shown by the following equation:

$$e_{cb}^- + O_2 \rightarrow O_2^{\bullet -} \quad (3.7)$$

At the same time, the positively charged electron "holes" can either be neutralized by OH^- groups or water molecules which produce $OH^\bullet$ radicals (Malato, 2002):

$$h_{vb}^+ + OH^- \rightarrow OH^\bullet + H \quad (3.8)$$

$$h_{vb}^+ + H_2O \rightarrow OH^\bullet + H^+ \quad (3.9)$$

Or direct oxidation with the organic reactant (R)

$$h_{vb}^+ + R \rightarrow R^{+\bullet} \rightarrow \text{degradation products} \quad (3.10)$$

As an example of the last reaction, holes can react directly with carboxylic acids generating CO_2:

$$RCOO^- + h_{vb}^+ \rightarrow R^\bullet + CO_2 \quad (3.11)$$

Also, the superoxide produced in equation (3.7) can further undergo neutralization by protons

$$O_2\bullet^- + H^+ \rightarrow HO_2\bullet \qquad (3.12)$$

The $HO_2\bullet$ will lead to the formation of hydrogen peroxide

$$2\ HO_2\bullet \rightarrow H_2O_2 + O_2 \qquad (3.13)$$

Next, the hydrogen peroxide, H_2O_2 may decompose into

$$H_2O_2 + e^- \rightarrow OH\bullet + OH^- \qquad (3.14)$$

The products would go back to reaction (3.8) and continue. These series of reaction lead to the generation of the extremely reactive hydroxyl radical, OH•. (Malato and Dibier, 2002) The hydroxyl radical, OH•, is a powerful oxidant (Lakeshmi et al, 1995). The hydroxide radical is a strong oxidizer, even stronger than the chlorine used as a sterilizer, hypochlorous acid, and ozone.

The overall reaction of the photocatalytic reaction can be represented by the following equation:

$$OH\bullet + \text{pollutant} + O_2 \rightarrow \text{products (CO2, H2O,...)} \qquad (3.15)$$

In the present study, when hydroxyl radicals are in contact with the Methylene Blue, the Methylene Blue can be ascribed to the cleavage of the bonds of the $C\text{-}S^+\text{=}C$ functional group

$$R\text{-}S^+\text{=}R' + OH\bullet \rightarrow R\text{-}S(\text{=}O)\text{-}R' + H^+ \qquad (3.16)$$

The product, R-S(=O)-R', can react further with the hydroxyl radicals to carbon dioxide, nitrate ions, ammonium ions and water as products in the reaction (Houas et al, 2001; Lakeshmi et al, 1995).

3.1.5 The Langmuir adsorption isotherm

According to several researchers (Malato and Dibier, 2002; Houas et al, 2001; Lakeshmi et al, 1995), the photocatalytic reaction of many organics, including methylene blue, were found to conform to a Langmuir adsorption isotherm. The Langmuir isotherm involves the following assumptions:

1. The surface is uniform
2. The adsorbed molecules form a monolayer
3. The adsorption-desorption equilibrium is comparable to that of the vaporization of a liquid.

If the adsorption of an adsorbate A on a site S is symbolized by

$$A + S \rightarrow AS \tag{3.17}$$

The rate of adsorption, r_a, is given by:

$$r_a = k_a P[S] \tag{3.18}$$

where k_a = the rate of constant of adsorption

P = partial pressure of A

$[S]$ = concentration of free sites

The rate of desorption, r_d, is given by:

$$r_d = k_d[AS] \tag{3.19}$$

where k_d = the rate of constant of desorption

$[AS]$ = concentration of occupied sites

Introducing the total concentration of sites $[S_o]$

$$[S_o] = [S] + [AS] \tag{3.20}$$

The coverage, θ, of the surface by A is defined as the ratio of:

$$\theta = [AS]/[S_o] \tag{3.21}$$

At equilibrium $r_a = r_d$, θ *can be rewritten as:*

$$\theta = KP/(1+KP) \tag{3.22}$$

where $K = k_a/k_d$ is the adsorption constant

Similar consideration can be made with liquids. For adsorption from a liquid phase, P is simply replaced by the concentration C of the considered adsorbate if the adsorption is nondissociative

$$\theta = KC/(1+KC) \tag{3.23}$$

When the isotherm of the photocatalytic activity resembles a Langmuir adsorption isotherm, the kinetics is of the Langmuir-Hingshelwood type and is characterized by (Pelizzetti and Serpone, 1989).

$$r = -\frac{dC}{dt} = \frac{kKC}{1+KC} \tag{3.24}$$

Where C = the concentration

k = the rate constant

K = apparent adsorption constant

A standard way of using equation (3.24) to plot the experimental data in the forms of the inverse initial rate versus inverse the initial concentration as expressed below:

$$\frac{1}{r} = \frac{1}{k} + \frac{1}{kK}\frac{1}{C} \tag{3.25}$$

where k and K can be obtained from the intercept and the slope of the line respectively.

In the area of water and wastewater treatment, the Langmuir-Hinshelwood equation can be simplified to a first-order expression since the concentration of reagent is usually low such that KC <<1. (Houas et al, 2001)

$$r = -\frac{dC}{dt} = kKC \tag{3.26}$$

The equation can be further simplified to:

$$-\frac{dC}{dt} = k'C \tag{3.27}$$

where $k' = kK$

Under this circumstance, the apparent reactivity is the product of two characteristics: its tendency to be converted when adsorbed, k, and its apparent adsorption constant, K. The constant, k', is very likely to be a function of illumination intensity, I. Hence comparisons between reactants can only be made when using the same catalyst and the same illumination sources. Also, factors like temperature, nature of the reactant, pH, wavelength of the incident light are likely to affect the k' value.

3.2.1 Electrolytic process

In an electrolytic cell as shown in Figure 3.4, two metal electrodes of a suitable metal, eg. platinum, are immersed in an aqueous solution of a salt, an acid or base, where these electrodes are connected to a direct current source, a current flows through the solution at a certain minimum voltage. Reactions take place at the same time at both electrodes. Solutions, which conduct electrical current are termed electrolytes, and the overall process which occurs at the electrodes is termed electrolysis. The positively charged ions in the electrolyte, the cations, migrate towards the cathode connected to the negative pole of the direct current source. The negatively charged ions, the anions, migrate towards the anode connected to the positive pole of the direct current source. (Raub and Muller, 1967)

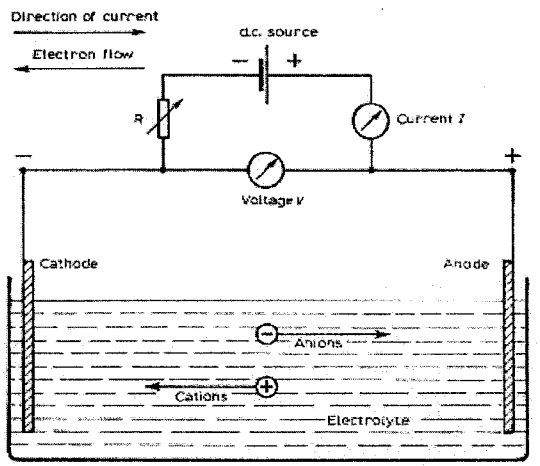

Figure 3.4 An Electroyltic Cell (Raub and Muller, 1967)

3.2.2 The Nerst Equation

The Nerst equation describes the relationship between the electrode potential and the concentration of the ionic species involved in the electrode reaction. The general form of the Nerst equation is written as follow: (Newman, 1991)

$$E_h = E_{h,n} + \frac{RT}{zF} \ln c_i \qquad (3.28)$$

where R = Gas constant = 8.31 8.31 m^3.Pa/mol.K

T = 298°K (=25°C)

F = Faraday number = 96500 coulomb

c_i = Initial concentration

E_h= potential

This potential, $E_{h,n}$, of an electrode in a solution having unimolar ion activity is known as the normal potential, ground potential or standard potential. A collection of these normal potentials, arranged in the order of their magnitude, gives the well-known electrochemical potential series as shown in the following table.

System	*Potential* $E_{h,N}$ *(volts)*	*System*	*Potential* $E_{h,N}$ *(volts)*
Au/Au^{+}	+1.7	Fe/Fe^{3+}	−0.036
Au/Au^{3+}	+1.42	Pb/Pb^{2+}	−0.126
$O_2/2H^{+}$	+1.23	Sn/Sn^{2+}	−0.140
Pt/Pt^{2+}	+1.2	Ni/Ni^{2+}	−0.23
Pd/Pd^{2+}	+0.83	In/In^{+}	−0.25
Pb/Pb^{4+}	+0.80	Co/Co^{2+}	−0.27
Ag/Ag^{+}	+0.799	In/In^{3+}	−0.34
Rh/Rh^{2+}	+0.6	Cd/Cd^{2+}	−0.402
Cu/Cu^{+}	+0.52	Fe/Fe^{2+}	−0.44
Cu/Cu^{2+}	+0.34	Cr/Cr^{3+}	−0.71
Sn/Sn^{4+}	+0.005	Zn/Zn^{2+}	−0.763
$H_2/2H^{+}$	+0.00	Al/Al^{3+}	−1.66
		Ti/Ti^{2+}	−1.75

Table 3.1 – Standard potential of various metals (Raub and Muller, 1967)

The practical application of the Nernst equation is subject to limitations, because, being a thermodynamic law, it applies only to the thermodynamics of a reaction. Catalytic effects, kinetic processes, overvoltages, reaction inhibitions, etc. can significantly alter the behavior of an electrode from the expected results on the basis of the Nernst equation.

3.2.3 Anodic Processes

In a bath containing an anode the oxidation reaction which gives rise to the passage of current at the anode consists of the emission of metal ions into the solution according to the following reaction:

$$M \rightarrow M^{z+} + ze^{-} \quad (3.29)$$

In the present project, the following reaction may occur:

$$2H_2O \rightarrow O_2 + 4H^{+2} + 4e^{-} \quad (3.30)$$

3.2.4 Cathodic processes

The cathodic processes can be summarized with the following general equation

$$M^{z+} + ze^{-} \rightarrow M \quad (3.31)$$

This is often accompanied by hydrogen deposition

$$2H^{+} + 2e^{-} \rightarrow H_2 \quad (3.32)$$

Other reactions may also take place at the cathode, such as

$$Fe^{3+} + e^{-} \rightarrow Fe^{2+} \quad (3.33)$$

In the present project, nickel and zinc ions were removed electrochemically as shown in the following reactions

$$Ni^{2+} + 2e^{-} \rightarrow Ni \quad (3.34)$$

$$Zn^{2+} + 2e^{-} \rightarrow Zn \quad (3.35)$$

3.2.5 Choice of materials for Anode and Cathode

General criteria in selection of materials for cathodes and anodes used in electrocells are:

- The cathode must be electrochemically stable at the pH range used to avoid corrosion
- The cathode and anode should have a high surface area per projected area
- The materials used for both the cathode and the anode must be economically feasible
- The anode should be coated with a thin layer of conductive material such as novel conductive polymer materials to prevent corrosion. Stainless steel electrodes did not corrode as much as tin or nickel electrodes.

For the present project, considering the above factors, the best material for the anode was stainless steel. Aluminum was used for the cathode due to the following reasons (Storrar, 2002):

1. Metals like platinum and gold are very expensive
2. Corrosion of nickel cathode was observed in previous studies. Nickel corroded in a study conducted by Eltech Systems Corporation
3. Aluminum has been proven to reduce both dissolved zinc and nickel in past studies at Ryerson University by other researchers. (Boithi, 2002)

3.2.6 Model for the electrochemical treatment

In electrochemical engineering, there are three major types of electrochemical reactors, which include batch reactors, continuous stirred reactors and plug flow reactors. In the present project a batch reactor with recycle (as shown in figure 3.5) was used.

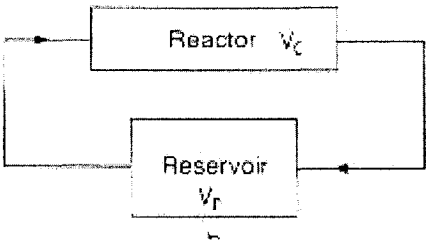

Figure 3.5 - Electrochemical Batch Reactor with Recycle

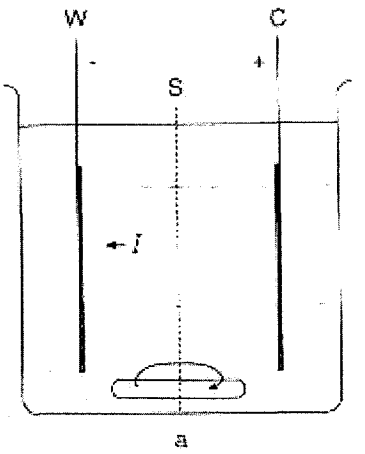

Figure 3.6 -Electrochemical Batch Reactor

According to Wendt and Kreysa (1999), the general electrode reaction could be modeled as

$$S + v_e e^- = P \tag{3.36}$$

where v_e is the stoichiometric coefficient of electrons. The number of moles produced at constant current, which provides a charge $Q=I\int t$, is given by:

$$n_p = -\frac{Q}{v_e F} = -\frac{I}{v_e F} t = -\frac{It}{v_e F} \tag{3.37}$$

If one takes the derivative with respect to time, t, the above equation can be rewritten as:

$$\frac{dn_p}{dt} = -\frac{1}{v_e F} I \tag{3.38}$$

Since the rate of charge transfer is proportional to the electrode area, by dividing both sides of equation the electrode area, A_e, the following equation is obtained:

$$\frac{1}{A_e}\frac{dn_p}{dt} = -\frac{1}{v_e F}\frac{I}{A_e} \tag{3.39}$$

where (I/A_e) is the current density, i. The above equation became:

$$\frac{1}{A_e}\frac{dn_p}{dt} = -\frac{1}{v_e F} i \tag{3.40}$$

Multiply both sides by A_e,

$$\frac{dn_p}{dt} = -\frac{A_e}{v_e F} i \tag{3.41}$$

By dividing both sides of the equation with volume, equation 3.41 could be expressed in terms of concentration as:

$$\frac{d\frac{n_p}{V_r}}{dt} = -\frac{i}{v_e F}\frac{A_e}{V_r} \tag{3.42}$$

$$\frac{dC_r}{dt} = -\frac{i}{v_e F}\frac{A_e}{V_r} \tag{3.43}$$

The term (i/v_eF) can be simplified to:

$$\frac{dC_r}{dt} = -k_m C_r \frac{A_e}{V_r} \tag{3.44}$$

Introducing variable, K

$$K = k_m \frac{A_e}{V_r} \tag{3.45}$$

Sub (3.46) into (3.45)

$$\frac{dC_r}{dt} = -KC_r \tag{3.46}$$

Equation 3.46 represents a 1st order decay of metal concentration in the solution. This model can be used to evaluate the performance of the electrolytic cell. Also, it can be integrated to give the following equation:

$$\ln\frac{C_t}{C_0} = -K(t_t - t_0) \tag{3.47}$$

Therefore, the concentration of the metal at time t can be expressed as:

$$C_t = C_0 \exp[-K(t_t - t_0)] \tag{3.48}$$

Alternatively, the above equation can be rewritten as:

$$C_0 - C_t = C_0\{1 - \exp[-K(t_t - t_0)]\} \tag{3.49}$$

$$m = m_0\{1 - \exp[-K(t_t - t_0)]\} \tag{3.50}$$

CHAPTER 4 - EXPERIMENTAL METHODOLOGY

4.1.1 Set up of the Apparatus

In the present study, the experiment was conducted in two modes of operation. The first one involved the study of the combined suspended photocatalytic and electrochemical treatment of a simulated wastewater containing organic matter and heavy metals. The effect of liquid flowrate, wavelength, and pH on the pollutant removal rate was investigated. The second mode of operation involved the study of the combined immobilized photocatalytic and electrochemical treatment of the same simulated wastewater.

An experimental apparatus as depicted in Figure (4.1a) & (4.1b) was used. It consists of:

1) Plastic storage tank (76cm long x 60cm wide x 45cm high)
2) ½ horsepower Jet pump
3) Cooling coils were installed at the bottom of the reactor to maintain the wastewater temperature at a constant level
4) An AC electric motor (Dayton Model #62081) was used to drive the rotating discs at 16RPM
5) A liquid flowmeter (Hedland Inc, Racine, WI, USA) was used to measure the liquid flowrate.
6) Three low pressure Mercury UltraViolet (UV) lamps were used to provide UV light.

Table 4.1 – Ultraviolet lamp characteristics

Description	Wavelength	Model #
254nm Ultraviolet Lamp	254nm	UVS-28
302nm Ultraviolet Lamp	302nm	UVM-28
365nm Ultraviolet Lamp	365nm	UVL-28

7) Rotating Discs – a)Suspended Operation mode. Four mixing paddles (20cm x 8cm) were attached to the two discs.

   b) Immobilized Operation mode. Four Immobilized TiO_2 plate (as described in Section 3.4) were attached to the two discs.

8) Electrolytic Cell – Consists of 6 metal strips of 316 Stainless steel and Aluminum (54cm long x 3.5cm wide)

4.1.2 Test equipment and reagents

1) Stirrer – The Thermalyne Magnetic Stirrer was used for dissolving powders like Methylene Blue, Titanium dioxide ....etc
2) Scales – The Scientech SA210D 3-digital scale was used for measurements of all components added to the wastewater.
3) Power Supply – The Hewlett Packard 6218A Power supply was used to provide the necessary current and voltage to the electrolytic cell
4) Colorimeter – The Orbeco-Hellige colorimeter (model 975-MP, Orbeco Analytical System, Inc, Farmingdale, New York) was used to measure the concentration of Zinc and Nickel ions in the sample

5) Spectrophotometer – The Ultraviolet/Visible Spectrophotometer (Perklin Elmer, Lambda 20) was used to measure the concentration of Methylene Blue in the sample

4.1.3 Reagents

1) Methylene Blue – Methylene Blue, Sigma Alderich M44907-100G CAS#61-73-4
2) Zinc Sulfate – Zinc, 7-Hydrate, Crystal, JT Baker.
3) Nickel Sulfate – Nickelous Sulfate, 6-hydrate, Crystal, JT Baker.
4) Potassium Sulfate – Potassium Sulfate, Crystal, A&K Petrochem.
5) Titanium Dioxide – Titanium Dioxide Degussa P-25. Stochem Inc, Brampton, Canada.

Figure 4.1 - SCHEMATIC DIAGRAM OF THE EXPERIMENTAL SETUP (Suspended TiO_2 Mode)

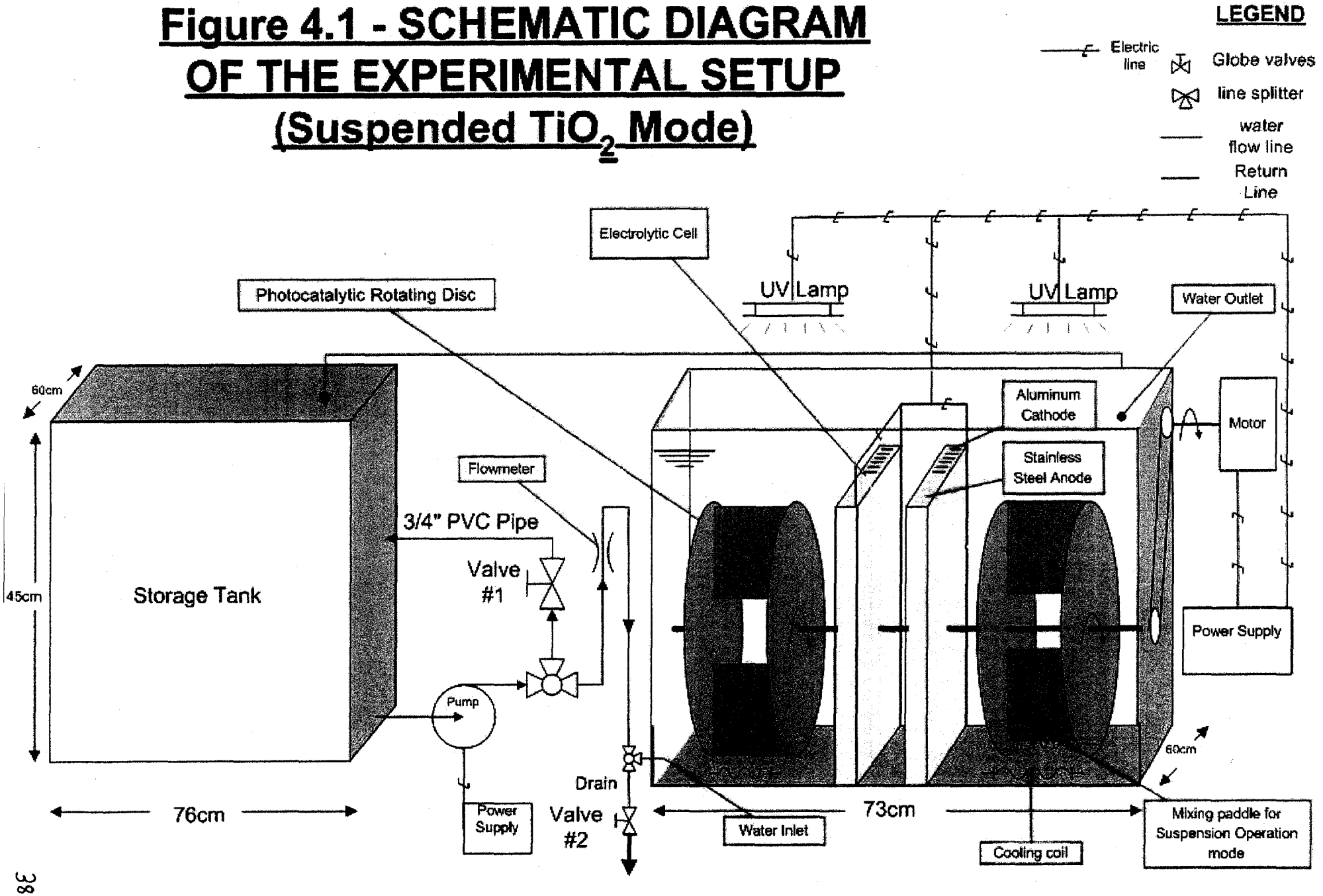

Figure 4.2 - SCHEMATIC DIAGRAM OF THE EXPERIMENTAL SETUP (Immobilized TiO_2 mode)

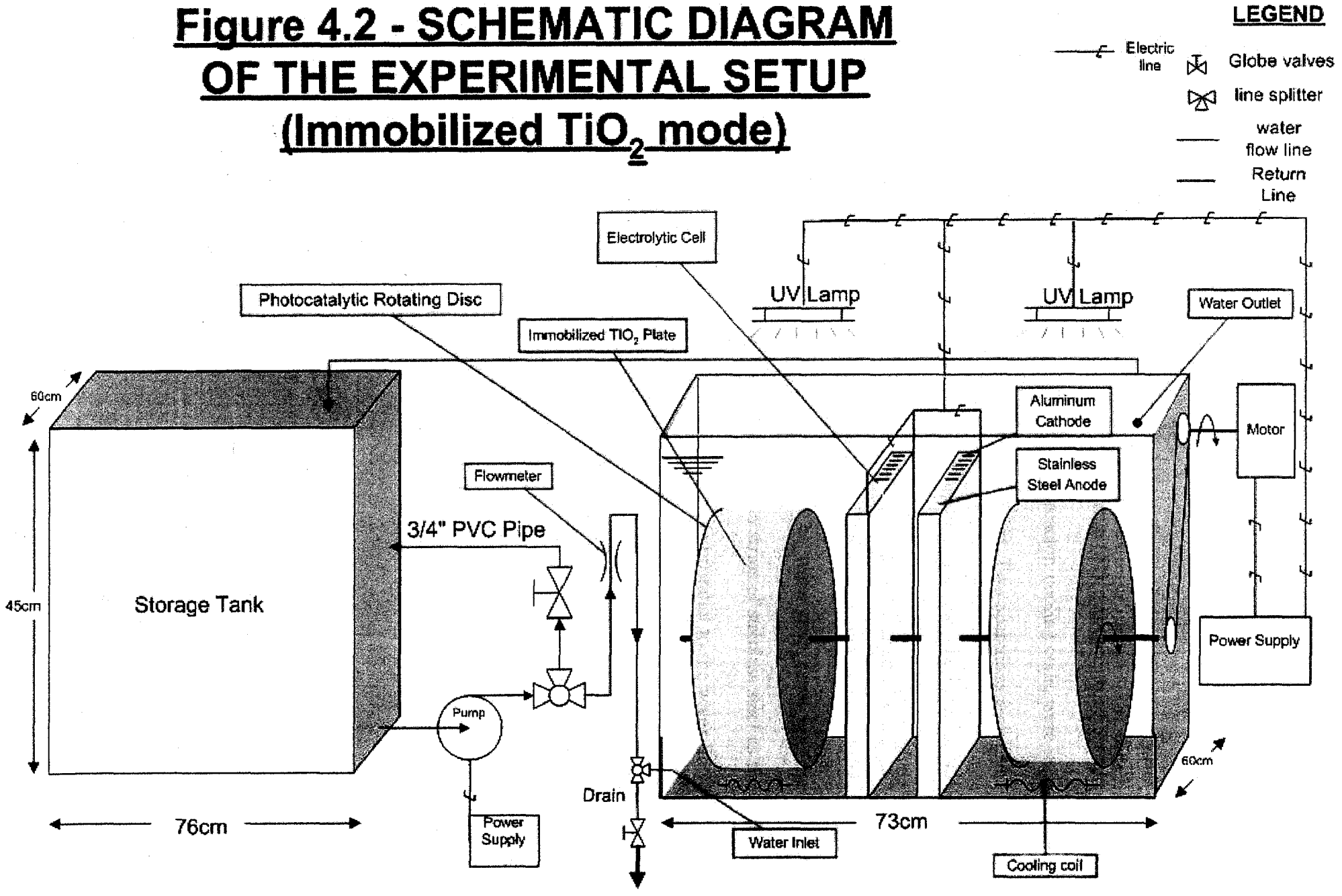

4.2 Flow of water through apparatus

For each cycle, the water was pumped out of the storage tank into the reactor by means of a jet pump. The flowing stream was split into a bypass line and through a flowmeter towards inlet at the bottom of the reactor. The bypass valve (#1) was used to adjust and maintain various water flow rates. At the bottom of the reactor, cooling coils, were used to maintain a constant temperature throughout the experiment. Two operations took place in the reactor, in the suspended photocatalytic operation mode, the ultraviolet lamps irradiated the titanium dioxide particles in water. In the immobilized photocatalytic operation mode, the ultraviolet lamps irradiated the immobilized titanium dioxide plates. This irradiation generated the photocatalytic reaction. The water then came into the electrocell region. The electrocell region is composed of 6 strips of stainless steel as the anode and 6 strips of aluminum metal as the cathode aligned parallel to the water flow. After that, the water flowed out of the reactor through an outlet at the top-side of the reactor and back into the storage tank, and then another cycle started over again.

4.3 Experimental Procedure

The following steps were followed for each experimental trial.

1. The experimental unit was cleaned with distilled water before each run. This is accomplished by running the system with distilled water for 24 hours.
2. The system was drained and the simulated wastewater was added to the tank. The composition of simulated wastewater was:

Distilled Water	320 Liters
Nickel Sulphate	40ppm
Zinc Sulphate	40ppm
Methylene Blue	1.1grams
Titanium Dioxide	20grams (for suspended photocatalytic operation mode)
Supporting electrode (Potassium Sulphate)	

3. The pump was started, the water flowrate was regulated using the bypass valve (#1). The heat exchanger, and the motor for the rotating discs were turned on.
4. After an hour of mixing, the ultraviolet lamps and the power supply the electrocell were turned on.
5. Samples were taken at 0, 24, 48 and 72 hours. The system was assumed to be well mixed. The samples were taken from the return line of the reactor as shown in figure 3.1
6. The concentration of Methylene Blue was determined by using a spectrophotometer.
7. Zinc and Nickel in mg/L were determined.

8. The system was turned off after 72 hours. The apparatus was thoroughly flushed with water. All residual at the bottom of the storage tank or reactor was vacuumed.

4.4 Determination of Methylene Blue concentration by Ultraviolet/Visible Absorption Spectrometry

The concentration of Methylene Blue was determined by absorbance using a UV/visible Spectrophotometer. (Perklin Elmer, Lambda 20) For the present study, most of the sample contained significant amount of titanium dioxide. Since titanium dioxide is white in color and it is not dissolved in water, the presence of titanium dioxide directly affect the measurement of absorbance by blocking the analyzing beam of the spectrophotometer which would give a higher absorbance reading. Therefore, the samples had been allowed to settle for 24 hours in the dark before measurements of Methylene Blue were carried out.

4.5 Calibration of the spectrophotometer for the determination of Methylene Blue concentration

The concentration of Methylene Blue is determined by measuring the absorbance using a spectrophotometer. According to the Beers Law, the concentration is related to the absorbance as:

$$\mathbf{A=\varepsilon bc} \qquad (5.1)$$

Where A is absorbance (no units, since $A = log_{10} P_0 / P$)
ε is the molar absorbtivity with units of L mol^{-1} cm^{-1}
b is the path length of the sample - that is, the path length of the cuvette in which the sample is contained.
c is the concentration of the compound in solution, expressed in mol L^{-1}

Samples of known concentration of methylene blue solutions were measured at 664nm wavelength and the data obtained is presented in table 5.1

Table 5.1 - Tabulated results for Absorbance vs Methylene Blue concentration

[MB] (PPM)	Absorbance
0	-0.0003
0.504	0.1254
1	0.2524
2.09	0.5134
2.532	0.6095
3.046	0.7233
3.514	0.8288
4.06	0.9334
25.18	1.9613
40.12	2.3595

The wavelength of 664nm was used because methylene blue has a peak absorption at this wavelength as shown in the plot of absorption scanning in appendix B. It is expected that the absorbance and concentration should be related linearly according to the Beers Law. However, at absorbance >1.0, the linear relationship did not apply. This was due to the

limitations of the Beer's Law. According to Skoog et al (1998), deviations from the direct proportionality between the measured absorbance and concentration are frequently encountered. At high concentrations, the average distance between the molecules is diminished to the point where each molecule affects the charge distribution of its neighbors. This interaction, in turn, can alter the ability of the molecules to absorb a given wavelength of radiation. For example, the molar absorptivity at 436nm for the cation of methylene blue in aqueous solution is reported to increase by 88% as the dye concentration increased from 10^{-5} to 10^{-2}M. (Skoog et al, 1998) Therefore, only data points with absorbance <1 were used for the calibration of Methylene Blue vs Absorbance as shown below.

Figure 4.1c –Absorbance vs Methylene Blue Concentration

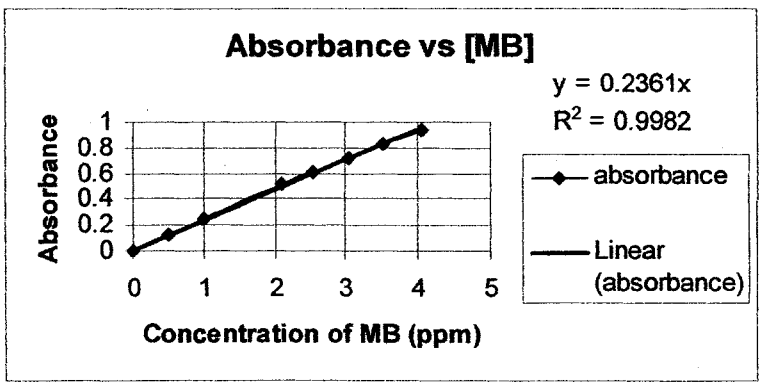

Using Microsoft Excel's linear regression, the following linear relationship between MB concentration and absorbance was obtained:

$$A = 0.2361[MB] \qquad (5.2)$$

This equation was used for the determination of the Methylene Blue concentration throughout the present study.

4.6 Determination of Zinc and Nickel concentration in the wastewater

The dissolved metals, Zn^{++} and Ni^{++}, were determined using a pre-calibrated colorimeter. (Orbeco – Helige Model 975-MP, Water Analysis system. Orbeco Analytical Systems, Inc, Farmingdale, New York.)

The colorimeter instructions were followed for Nickel Test #41 and Zinc Test #27, as provided by the manufacturer. These tests are included in Appendix C. By using uncertainty analysis, the uncertainty of the percentage removal of nickel is found to be 6.1%. In section 5.3, after 72 hours of treatment, the percentage removal of nickel is 67.0 ± 6.1 %. Similarly, by using uncertainty analysis, the uncertainty of the percentage removal of zinc is found to be 9.1%. In section 5.3, after 72 hours of treatment, the percentage removal of zinc is 63.4 ± 9.1 %.

4.7 Immobilization procedure of the titanium dioxide

In photocatalytic water treatment the difficulty of the commercialization of the photocatlytic oxidation method in water wastewater treatment stems basically from the fact that the post-treatment removal of the semi-conductor materials utilized as the photocatalyst causes a significant off-set in the benefits of the photocatalytic mineralisation process. The problem is due to the small particle size of the photocatalyst. To solve this problem, numerous immobilization methods have been tested. A report written by Pozzo et al (1997) provided a summary of the commonly used immobilized methods. A binding material is usually used to physically bond the titanium powder to a supporting material. Two conditions must be satisfied for the process to be feasible in photocatalysts onto supports: A good adherence catalyst/support, and nondegradation of the catalyst activity by the attachment process (Skelton and Fabiyi, 2000).

The following section outlines the steps of the immobilization method used in the present study:

1. 4 plates (48cm long x 16.5cm wide) were cut out of a polycarbonate sheet. According to Kwon et al (2004), polycarbonate sheet is a good supporting material for photocatalyst as it exhibit minimum amount of decomposition by UV light.
2. A plastic mesh was glued firmly to the polycarbonate plate with acrylate solvent (containing Methylene chloride, Trichloroethylene, Methyl Methacrylate Monomer. IPS corporation, Gardena, CA) as shown in figure 4.2:

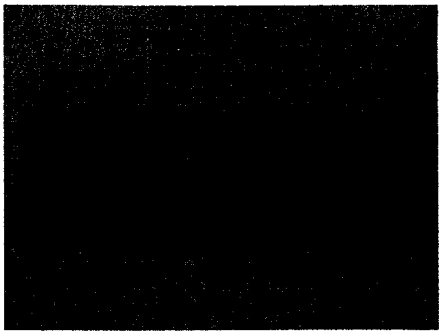

Figure 4.2 – Polycarbonate sheet

The objective of adding the plastic mesh was to increase the surface area for the attachment of the binding material and the titanium dioxide.

3. A thin layer of PVC glue (binding material) was applied on top of the polycarbonate plate.
4. Titanium dioxide powder was then sprinkled on top of the plate immediately after step 3 as shown in figure 4.3. It is important that the powder is sprinkled as fast as possible since the PVC glue dries quickly.

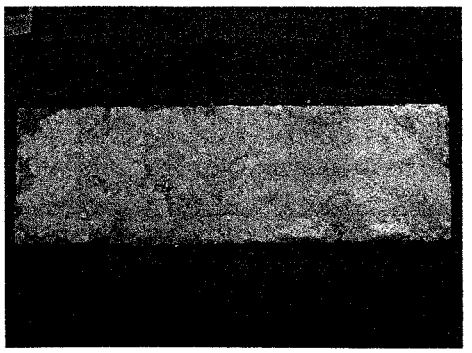

Figure 4.3 – Unfinished immobilized titanium dioxide plate

5. Applied light pressure onto the titanium dioxide layer to ensure the titanium dioxide powder "stick" with the PVC glue.

6. The plates was placed in a ventilated place to dry at room temperature for 24 hours (Figure 4.4). The plates were then placed to a water bath for at least 3 hours to remove the unattached titanium dioxide.

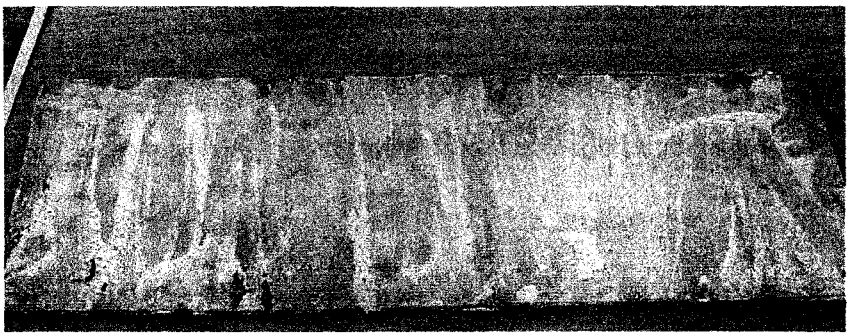

Figure 4.4 – Immobilized titanium dioxide plate

7. The titanium dioxide was taken out of the water bath and ready for use as shown in figure.

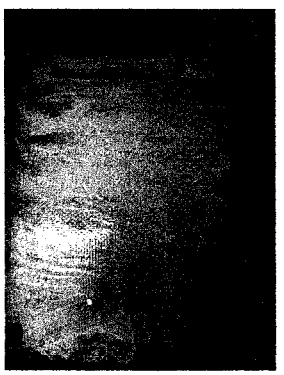

Figure 4.5 – Used titanium dioxide plate

CHAPTER 5 – RESULTS AND DISCUSSIONS

5.1 Photocatalytic treatment of Methylene Blue, Nickel and Zinc with suspended titanium dioxide

One of the first objectives of the present study is to investigate the effect of photocatalytic treatment on water constituents with suspended titanium dioxide. To study the effectiveness of the suspended photocatalytic treatment for organic matter, the percentage removal of Methylene Blue was measured at 0 hours, 24 hours, 48hours and 72 hours and tabulated in the table 5.1:

Table 5.1 – Percentage Removal of Methylene Blue in suspended photocatalytic treatment

Treatment Time (hours)	Absorbance	[MB] (mg/L)	[MB} % Removal
0	0.718	3.04	0.0
24	0.584	2.47	18.7
48	0.541	2.29	24.7
72	0.459	1.94	36.1

The variation of the removal of Methylene Blue with treatment time is presented on Figure 5.1

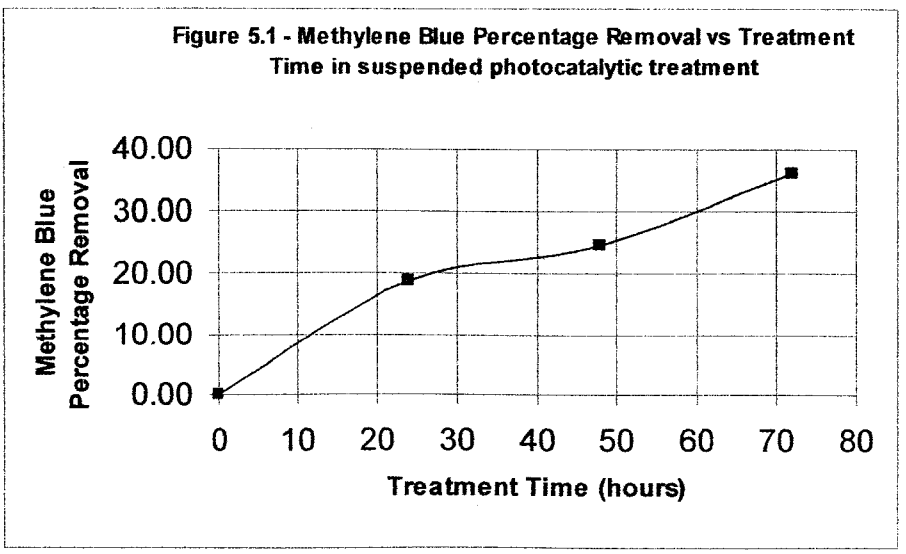

As shown in Figure 5.1, the irradiated suspended titanium dioxide by UV lamp was capable to mineralize organic matter such as Methylene Blue using the apparatus developed in the present study. The percentage removal of Methylene Blue increased with the treatment time. Due to the low percentage removal rate (36% in 72 hours), and the low number of data points (4 data points), it is difficult to conclude whether the removal rates exhibit first order or zero order removal.

In the present study, Zinc and Nickel were used as the model heavy metal ions. Semiconductor photocatalysis was reported to be able to eliminate certain types of heavy metals such as: gold, platinum and mercury (Schiavello M, 2001). Thus, the percentage removal of Zinc and Nickel was investigated under photocatalytic treatment and the results obtained are tabulated in Table 5.2 and plotted in Figure 5.2

Table 5.2 – Zinc and Nickel Percentage Removal vs Treatment Time in suspended photocatalytic treatment

Time	Zinc % Removal	Nickel % Removal
0	0.00	0.00
24	1.85	-0.72
48	7.04	3.24
72	4.07	2.64

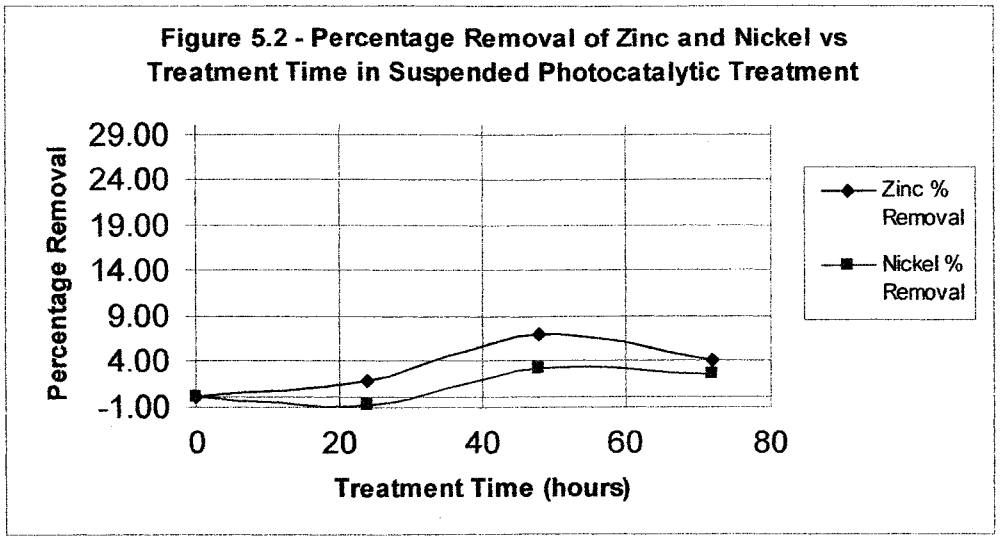

From Figure 5.2, it is observed that the photocatalytic treatment has insignificant effect on the removal of the dissolved zinc and nickel metals after 72 hours of treatment. It is believed that:

1) Photocatalytic treatment for heavy metal ions is only effective on some specific types of heavy metals. In the present study, the photocatalytic treatment has no effect on zinc and nickel ions. According to a study by Ray, semiconductor photocatalysis is unable to remove nickel ions. (Chen and Ray, 2001)

2) The applied light intensity ($0.5kW/cm^2$) does not provide enough energy to reduce the nickel and zinc ions into metals. A detailed explanation is given in section 5.7.

5.2 Photocatalytic treatment of Methylene Blue, Nickel and Zinc with immobilized titanium dioxide

As stated in the experimental section, titanium dioxide, the photocatalyst, was immobilized onto the polycarbonate sheets, which was the supporting material, by a binding material, PVC cement. Refer to the experimental section for the immobilization procedures.

After 72 hours of treatment, percentage removal of Methylene Blue, Nickel and Zinc was determined and tabulated in Table 5.3:

Table 5.3 – Methylene Blue, Zinc and Nickel Percentage Removal vs Treatment Time in immobilized photocatalytic treatment

Treatment Time (hours)	MB % Removal	BLANK	Zinc % Removal	Nickel % Removal
0	0.00	0	0.00	0.00
24	5.69	0.5	4.89	2.22
48	9.64	1.1	1.50	1.40
72	14.89	1.7	6.77	3.39

The change of organic matter by the Rotating Photocatalytic Reactor can be investigated by plotting the percentage removal of Methylene Blue vs Treatement Time:

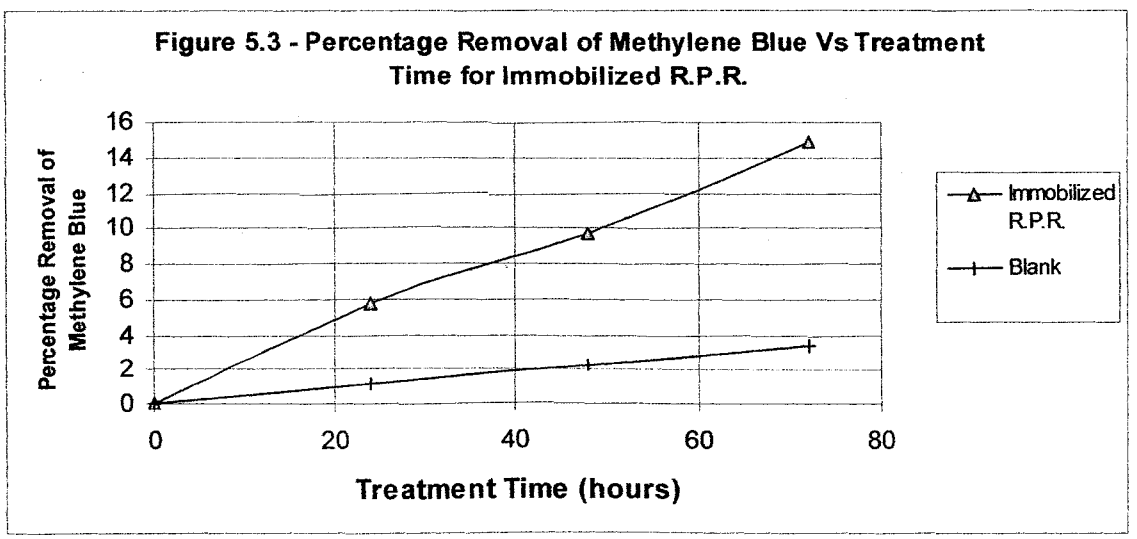

The blank experimental trial was defined as an experiment with the same operating parameters as the one being compared without the photocatalyst, titanium dioxide, and no voltage through the electrocell. With the absence of the photocatalyst, titanium dioxide, there was a slight percentage reduction (1.7%) of Methylene Blue after the experiment was run for 72 hours.

Figure 5.3 shows that the immobilized is effective for the treatment of Methylene Blue. Although the rate of removal is low (15% in 72 hours), significant amount of methylene blue can be decolorized after extended period of treatment. However, no significant reduction for dissolved zinc and nickel is observed as shown from figure 5.4. Any removal is believed to be contributed to the experimental error throughout the experiment as described in the error section.

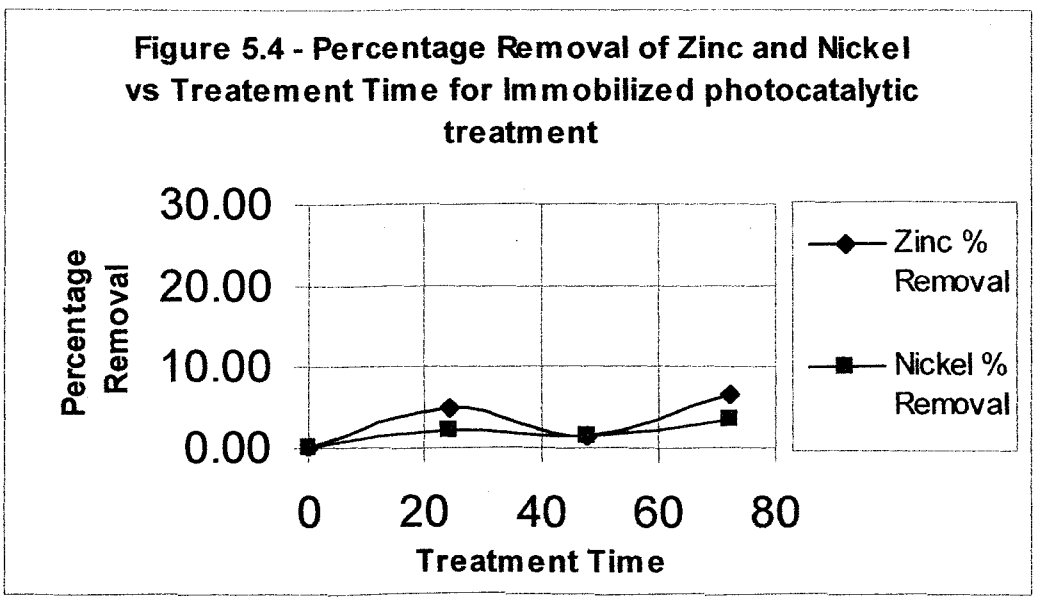

5.3 Electrochemical treatment of Methylene Blue, Zinc and Nickel

The electrochemical technology, which is well known as "a clean method of wastewater treatment", has lots of advantages (An et al, 2002). The ability to retrieve precious metals from dilute solutions and eliminate unwanted toxic metals stimulated research on this technology. In the present study, the role of electrochemical treatment was to remove dissolved Zinc and Nickel ions from the wastewater. The results on the electrochemical treatment of wastewater containing Nickel and Zinc are presented in tables 5.4 and 5.5 and plotted in Figure 5.5 as:

Table 5.5 – Percentage Removal of Zinc by electrochemical treatment

Time	Colorimeter Reading	Concentration(mg/L)	Percentage	Zinc % Removal
0	3.06	45.9	100.0	0.0
24	2.15	32.3	70.3	29.7
48	1.75	26.3	57.2	42.8
72	1.12	16.8	36.6	63.4

Table 5.6 – Percentage Removal of Nickel by electrochemical treatment

Time	Colorimeter Reading	Concentration(mg/L)	Percentage	Nickel % Removal
0	9.13	36.52	100.000	0.000
24	7.01	28.04	76.780	23.220
48	4.76	19.04	52.136	47.864
72	3.01	12.04	32.968	67.032

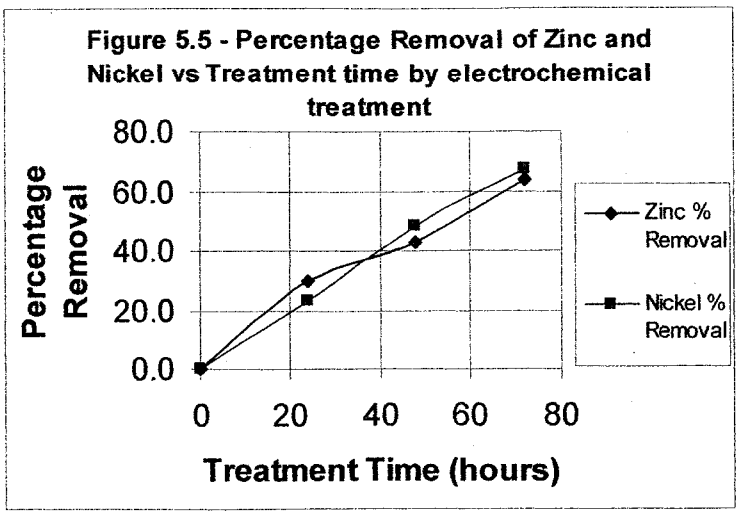

Figure 5.5 shows that the electrochemical treatment is effective for the elimination of Nickel and Zinc ions as more than 50% of the dissolved metals were removed in 72 hours. The error bars for the percentage zinc removal was found to be ±9% using 2 standard deviations of 6 measurements. Similarly, the error bars for the percentage zinc removal was found to be ±6% using 2 standard deviations of 6 measurements.

The standard reduction potential for Nickel ion, Ni^{2+}, is -0.23V, which is higher than that of -0.76V for Zinc ion, Zn^{2+} (Atkins, 1986). It was thus expected that Ni^{2+} would be removed more readily from the electrolyte than Zn^{2+} (Doan et al, 2003). However, Roventi et al reported that in the presence of Ni^{2+} in the electrolyte, Zn^{2+} co-deposited with Ni^{2+} at a lower potential than that for pure Zn^{2+} deposition. (Roventi et al, 2000). Nevertheless, in the present study as shown by the error bars in figure 5.5, no significant difference is observed between the rate of deposition of zinc and rate of deposition of nickel.

Not only the method of electrochemical deposition is capable to remove the amount of toxic metal ions in wastewater, it is also known to be effective for several organic and toxic pollutants (Vlyssides et al, 2000). Based on this fact, the removal of Methylene Blue by electrochemical treatment was examined and plotted in figure 5.6.

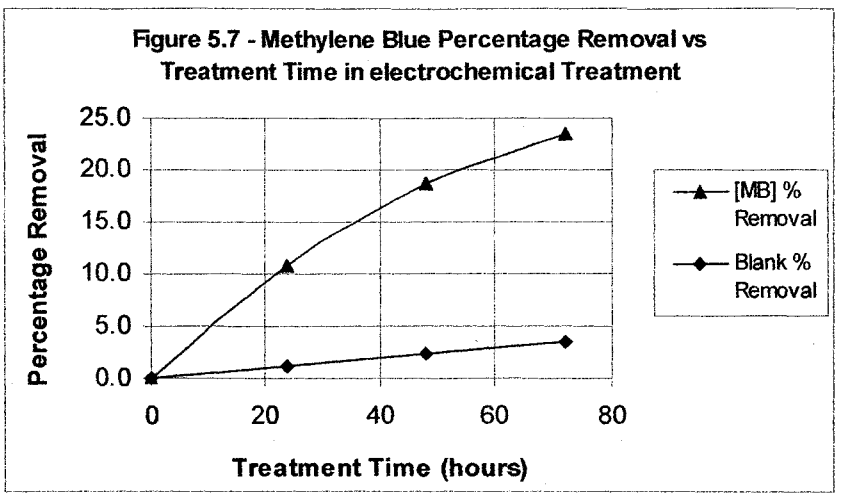

After 72 hours of electrochemical treatment at a current of 200mA, Methylene Blue concentration was reduced by 23.5%. This demonstrated that a significant amount of Methylene Blue was removed by the electrochemical treatment as compared to 3.5% removal without an external current. Similar observation were reported by with other researchers (Gulyas, 1997; Dziewinski et al, 1998).

5.4 Effect of combined Electrochemical and Suspended Photocatalytic Treatment of Methylene Blue, Zinc and Nickel

The major focus of the present study is to investigate the combined Photocatalytic and Electrochemical Treatment of the organic matter and metal ions in water. The preceding sections demonstrated the individual effect of Suspended Photocatalytic, Immobilized Photocatalytic and Electrochemical technique for the reduction of Methylene Blue, Zinc and Nickel ions in the simulated wastewater. To investigate the combined effect, an experiment using both suspended photocatalyic and electrochemical treatment was performed and the results obtained are tabulated in the following table:

Table 5.6 – Percentage Removal of Methylene Blue, Zinc and Nickel in the combined treatment

Time(hours)	MB % Removal	Zinc % Removal	Nickel % Removal
0	0.00	0.00	0.00
24	13.80	24.53	29.16
48	31.13	52.83	50.84
72	46.11	69.81	65.54

Culminating the results of the above table, the following table summarizes the individual and combined effects of the Immobilized, Suspended Photocatalytic and Electrochemical treatment on the removal of Methylene Blue, Zinc, and Nickel ions after 72 treatment hours.

Table 5.7 Individual and combined effects of photocatalytic and electrochemical treatment after 72 treatment hours

	UV light Intensity	Electrocell Voltage & Current	MB % Removal	Zinc % Removal	Nickel % Removal
Blank (No Treatment)	0	0	3.39	4.87	3.38
Suspended Photocatalytic treatment	0.5mW/cm^2	0	36.07	4.07	2.64
Immobilized Photocatalytic treatment	0.5mW/cm^2	0	14.89	6.77	3.39
Electrochemical Treatment	0	6V & 200mA	23.54	63.4	67.03
Combined Suspended Photocatalytic & Electrochemical Treatment	0.5mW/cm^2	6V & 200mA	46.11	69.81	65.54

Experiments, from which the data obtained are presented in table 5.7, were performed using the following experimental parameters:

Table 5.8 – Operating parameters for Section 5.3-5.6

Wastewater Volume	320L
Flowrate	24L/min
Temperature	24-25°C
pH	5.5-6.0

Based on table 5.8 and observations described in the previous sections, the following points can be drawn for 72 hours of treatment:

- Both Suspended and Immobilized Photocatalytic treatment were effective for treating Methylene Blue
- Both Suspended and Immobilized Photocatalytic treatment were ineffective for treating Zinc or Nickel ions
- Electrochemical Treatment was effective for treating Methylene Blue, Zinc and Nickel ions.
- No difference was observed between the percentage removal of Zinc ions and nickel ions in all treatments
- Suspended Photocatalytic treatment for Methylene Blue appeared to be more effective than the Immobilized Photocataltytic treatment. This is attributed to the much larger catalyst surface area in suspended titanium dioxide particles

The results on the percentage removal of Methylene Blue, Zi^{2+} and, Ni^{2+} with the treatment time for the combined suspended photocatalytic and electrochemical treatment are plotted in the figures 5.8 to 5.10.

Figure 5.8 - Comparsion of the combined effect of Suspended Photocatalytic & Electrochemical Treatment to other methods on the removal of Methylene Blue

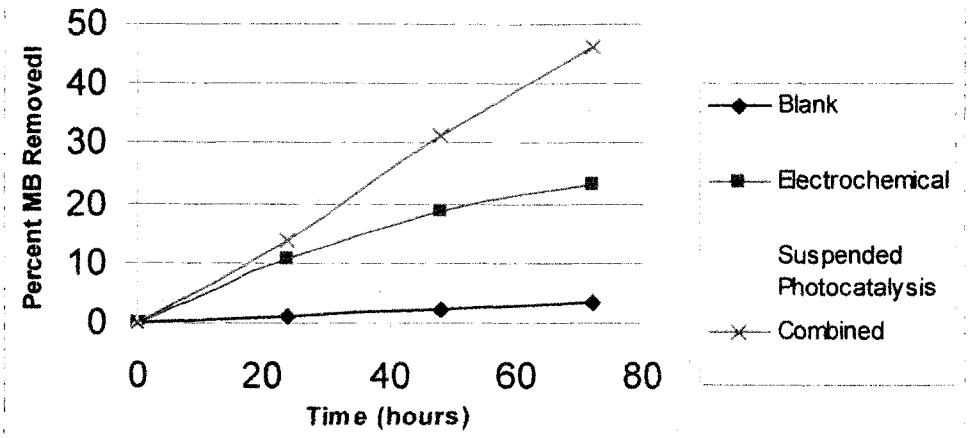

Figure 5.9 - Comparsion of the combined effect of Suspended Photocatalytic & Electrochemical Treatment to other methods on the removal of Zn^{2+}

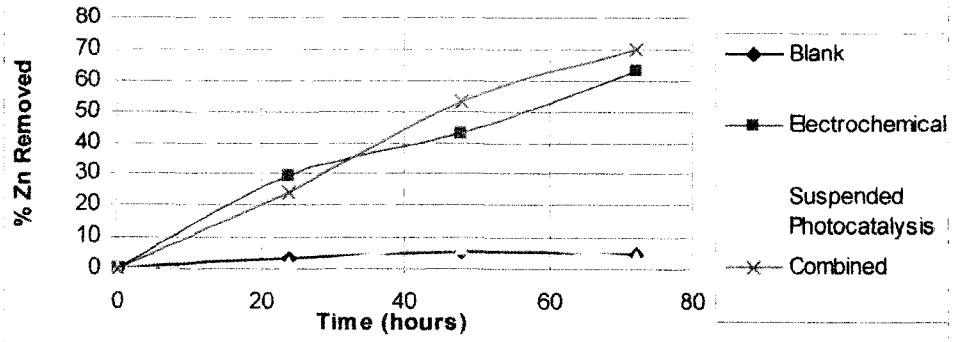

Figure 5.10 - Comparsion of the combined effect of Suspended Photocatalytic & Electrochemical Treatment to other methods on the removal of Ni2+

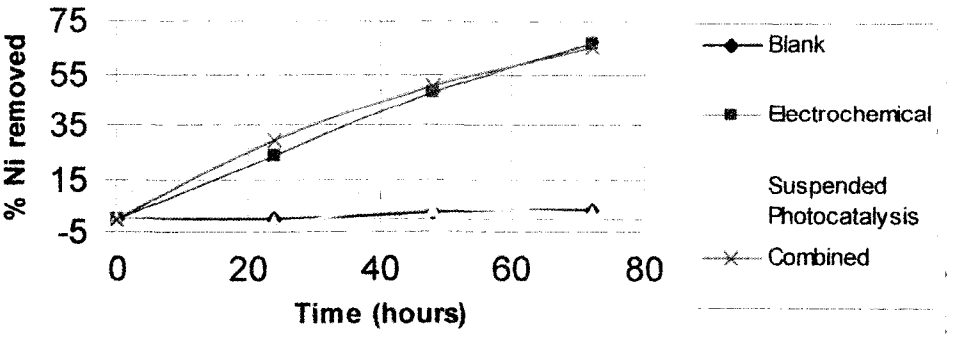

Similar trends were observed with the treatment using individual effect, i.e. electrochemical or photocatalytic effect only and the combined Immobilized Photocatalytic and Electrochemical Treatment on the removal of Methylene Blue, Zinc and Nickel ions as shown in Figures 5.11, 5.12 and 5.13.

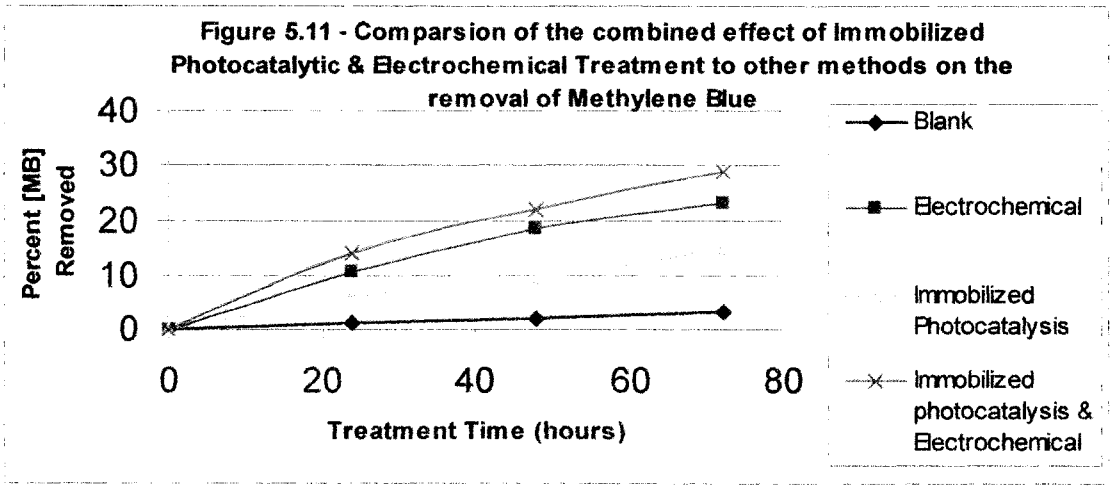

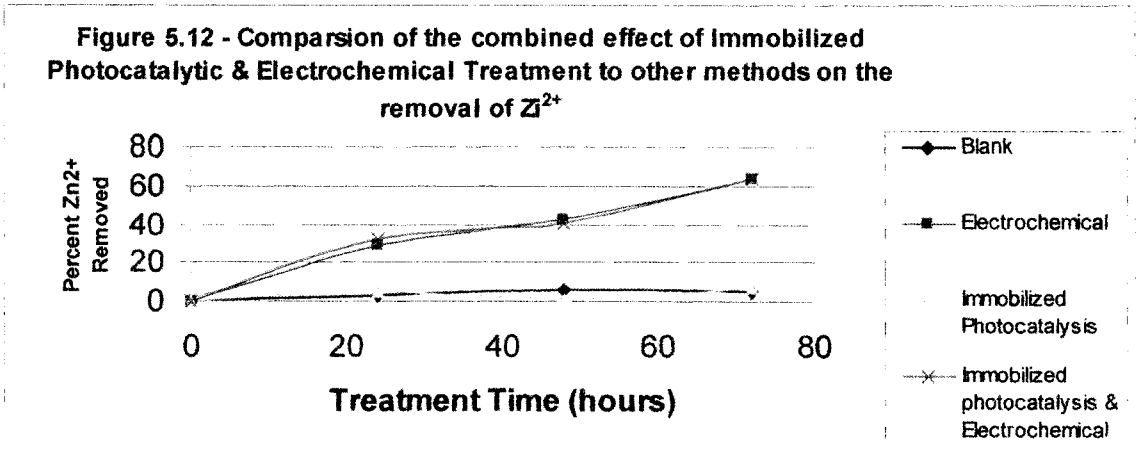

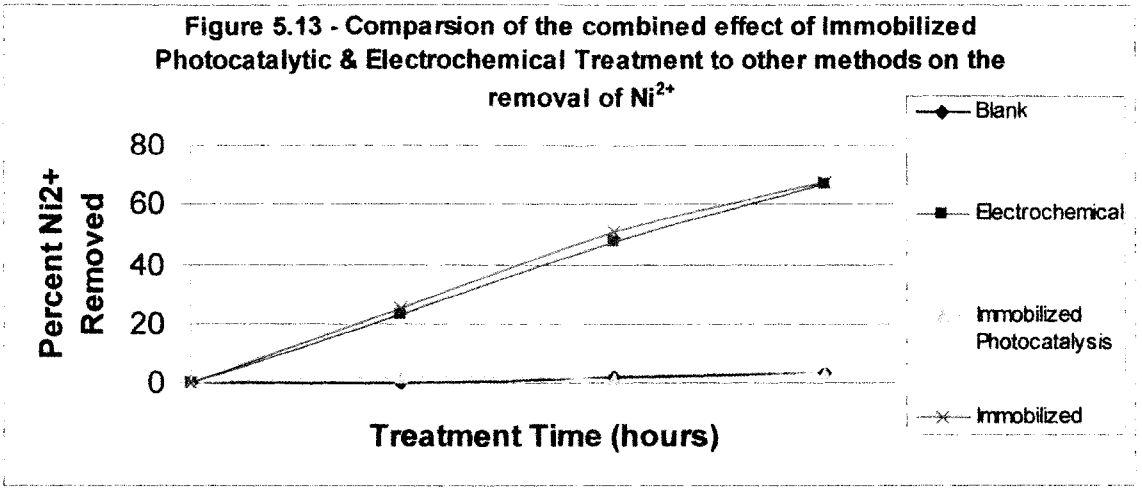

There was a synergy effect on the treatment of Methylene Blue when the photocatalytic and electrochemical method were used simultaneously. After 72 hours of treatment, the percentage removal of Methylene Blue in the combined Suspended Photocatalytic and Electrochemical method was 46.1%, while it was only 36.1% for the Suspended Photocatalytic method and 23.5% for the electrochemical method alone. The same observation was noted for the Immobilized Photocataltyic method, where the percentage of Methylene Blue in the combined Immobilized Photocatalytic and Electrochemical method was 28.9%, while it was only 14.9% for the Immobilized Photocatalytic method and 23.5% for the electrochemical method. It is believed that this enhancement effect is due to 3 major reasons: 1) Influence of iron species on the photoactivity of aqueous suspensions of titanium dioxide. 2) Reduction of recombination process of the electron-hole pair by the external electric field. 3) The anodic oxidation of organic by the external current.

The photoreactivity was known to be strongly influenced by some inorganic species in the reacting system (Schiavello, 1987). One such species is the iron, Fe^{2+} & Fe^{3+}, ions. (Mrowetz and Selli, 2003). In the present study, it is believed that iron ions

were generated by anodic corrosion of the anode at the electrocell. When suitable amounts of iron ions are present, some processes having beneficial influence on the photoreaction can occur. Among them, the most relevant reactions are:

$$Fe^{3+} + e^-_{(cb)} \rightarrow Fe^{2+} \quad (5.1)$$

$$Fe^{2+} + HO_2\bullet_{(surf)} + H^+_{(aq)} \rightarrow Fe^{3+} + H_2O_{2(surf)} \quad (5.2)$$

$$Fe^{2+} + H_2O_{2(surf)} + H^+_{(aq)} \rightarrow Fe^{3+} + OH\bullet + H_2O \quad (5.3)$$

$$H_2O_{2(surf)} + e^-_{(cb)} \rightarrow OH^- + OH\bullet \quad (5.4)$$

In reactions (5.1-5.4), Fe^{3+} behaves as cocatalyst and mediator. Fe^{2+} ions produced according to reaction (5.1) react with photo-produced H_2O_2 and/or peroxide radicals according to reactions (5.2) and (5.3). These last species can be photo-produced on the surface of the catalyst according to the following reactions:

$$O_{2(ads)} + e^-_{cb} + H^+_{(aq)} \rightarrow HO_2\bullet_{(surf)} \quad (5.5)$$

$$HO_2\bullet_{(surf)} + e^-_{cb} + H^+_{(aq)} \rightarrow H_2O_2 \quad (5.6)$$

By taking into account all the reactions described above, the concentration of OH• radicals, i.e. the primary oxidant species of the photodegradation process, increased. These increased hydroxyl radicals, as mentioned in the theory section, would be able to oxidize organic matters like Methylene Blue.

The second possible cause of the enhancement effect for the combined photocatalytic and electrochemical treatment is the reduction of the recombination of the electron-hole pairs at the catalyst surface. It has been repeatedly confirmed that the external electric field could enhance greatly photocatalytic efficiency, which is well known as an electric field enhancement of synergetic effect (An et al, 2002; Pelegrini et

al, 1999). As described in the theory section, after the photocatalyst is excited, the electron-hole pair can subsequently evolve in different pathways (Schiavello, 1997):

1. They can recombine with emission of thermal energy and/or luminescence. The electrons and holes can recombine as (Malato and Dibier, 2002):

$$e_{cb}^{-} + h_{vb}^{+} \rightarrow TiO_2 + \text{energy (heat)} \qquad (5.10)$$

   With the combination of the electrochemical technique, the external applied bias drives away the accumulated electrons via the external current, thereby promoting the selective oxidation of the dye on the TiO_2 surfaces. Therefore by reducing the recombination pathway, the desired, 2nd pathway increases.

2. React with electron acceptor or donor species giving rise to reduction and oxidation processes, respectively.

3. The final cause of the enhancement effect for the combined phtocatalytic and electrochemical treatment is the anodic oxidization of organic material. As described in section 5.3, Methylene Blue, which was the model organic used in the present study, was reduced by the electrochemical treatment after 72 hours of treatment.

5.5 The Kinetic constant for Photocatalytic Treatment of Methylene Blue

As mentioned in the theory section, the photocatalytic reaction with many organics, including methylene blue, were found to conform to a Langmuir absorption isotherm as

$$r = -\frac{d\,C}{d\,t} = \frac{kKC}{1+KC} \tag{5.8}$$

In the area of water and wastewater treatment, the Langmuir-Hinshelwood equation can be simplified to a first-order expression since the concentration of reagent is usually low such that KC <<1 (Houas et al, 2001).

$$-\frac{d\,C_t}{d\,t} = k'C \tag{5.9}$$

where k' = kK = decay rate constant

The above equation can be integrated to:

$$ln\left(\frac{C_t}{C_o}\right) = -k't \tag{5.10}$$

where C_t = concentration of Methylene Blue at a give time t

C_0 = initial concentration of Methylene Blue in the batch

k'= decay rate constant

In previous sections, all experiments were performed in 72 hour period. Since a sample was acquired in 24 hours, only 4 data points was available. In order to study the trend of the removal of Methylene Blue vs treatment time, more data points were required. Therefore, a run of 162 hours of suspended photocatalytic was performed and the fraction of Methylene Blue remaining in the holding tank with treatment time is plotted in Figure 5.14

Figure 5.14 – Fraction of Methylene Blue remaining vs Treatment Time for suspended photocatalytic treatment after 162 hours of treatment

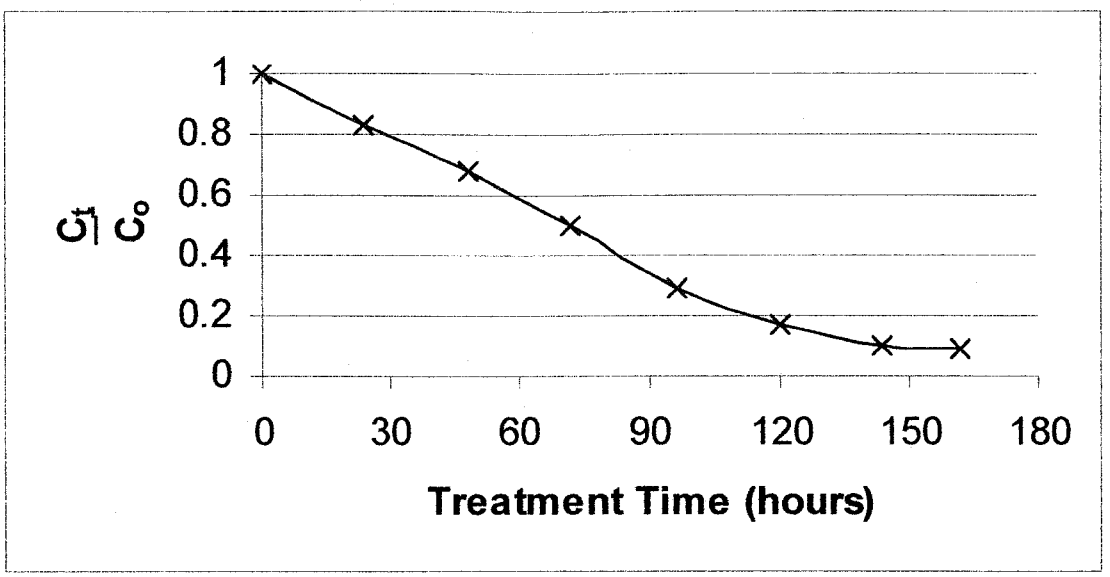

As shown in Figure 5.14, the concentration profile of Methylene Blue show an exponential decay in the batch, which coincided with the Langmuir-Hinshelwood equation at low concentration. In order to determine the decay rate constant, k', a plot of $-\ln(C_t/C_0)$ vs t had to be plotted as shown below:

Figure 5.15 – Determination of the decay rate constant for Methylene Blue

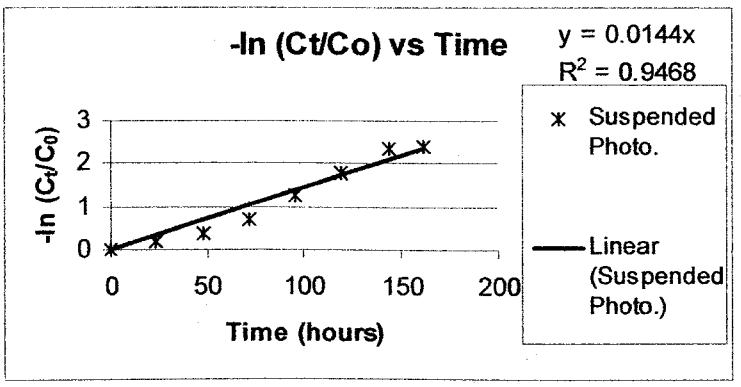

Using linear regression, k' was found to be 0.0144 h^{-1}. Similarly, this model was applied to the immobilized photocatalytic process and the decay rate constant was found to be 0.0022 h^{-1}. However, when the rate constants were compared to similar experiments by other researchers, the suspended and immobilized photocatalytic decay rate constant

appeared to be much smaller than those found in the present study as shown by the table 5.10. This was primarily due to the different process parameters used in the present study. To demonstrate the contribution of the specific process parameters, the specific decay rate constant, k" can be defined as:

$$k' = k'' \frac{A_{sac}}{V} \tag{5.11}$$

Where k' = decay rate constant ($hour^{-1}$)

A_{sac} = Surface area of the photocatalyst (m^2)

V = Wastewater volume

Therefore, by taking the volume of wastewater, surface area of the photocatalyst into account, it was observed that the results obtained in the present study are comparable to other researchers as shown in table 5.9. Further, the specific rate constant is directly related to the light intensity.

Table 5.9 Comparison of decay rate constants with other researchers

	Decay Rate Constant, k'	Wastewater Volume	Light Intensity	Specific Rate Constant, k"
Suspended Photocatalysis in the present study	$0.0144hr^{-1}$	320L	0.5 mW/cm2	$0.073 L/m^2.hr$
Suspended Photocatalysis by RAJESHWAR et al, 1999	$4.65hr^{-1}$	1L	1.0 mW/cm2	$0.093 L/m^2.hr$
Immobilized Photocatalysis in the present study	$0.0022hr^{-1}$	320L	0.5 mW/cm2	$2.34 L/m^2.hr$
Immobilized Photocatalysis by Kuo et al, 2000	$0.456hr^{-1}$	8L	3.0 mW/cm2	$14.59L/m^2.hr$

5.6 The Effect of flowrate on the removal of Methylene Blue, Zinc and Nickel ions by combined photocatalytic and electrochemical treatment

Liquid velocity influences both the mass transfer rate of metal ions from the electrolyte to the electrodes, and the mass transfer rate of organic matter from the bulk to the surface of the photocatalyst, titanium dioxide. In the present study, experiments with various liquid flowrate of 8, 16, 24, and 24 Liters per minute were performed to study the effect of flowrate for Methylene Blue, Zinc and Nickel ions by combined photocatalytic and electrochemical treatment. The results obtained are tabulated in the following tables and plotted in Figures 5.16 to 5.18.

Table 5.10 – Effect of flowrate in combined treatment for Methylene Blue

Methylene Blue	Flowrate			
Time	8	16	24	32
0	0.00	0.00	0.00	0.00
24	14.39	13.80	16.78	12.25
48	29.07	31.13	31.51	27.13
72	44.49	42.73	49.93	41.87

Table 5.11 – Effect of flowrate in combined treatment for Zn^{2+}

Zinc	Flowrate			
Time	8	16	24	32
0	0.00	0.00	0.00	0.00
24	33.19	26.25	24.53	29.70
48	52.50	45.94	52.83	56.15
72	63.17	68.35	69.81	65.33

Table 5.12 – Effect of flowrate in combined treatment for Ni^{2+}

Nickel	Flowrate			
Time	8	16	24	32
0	0.00	0.00	0.00	0.00
24	33.35	27.90	29.16	30.50
48	46.15	50.87	50.84	52.25
72	62.17	60.31	65.54	68.86

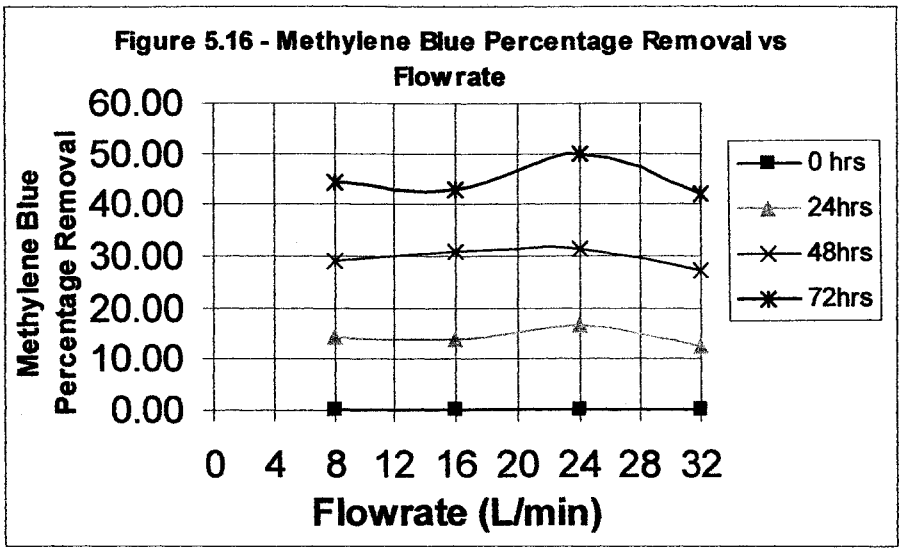
Figure 5.16 - Methylene Blue Percentage Removal vs Flowrate
Methylene Blue Percentage Removal
60.00
50.00
40.00
30.00
20.00
10.00
0.00
0 4 8 12 16 20 24 28 32
Flowrate (L/min)
0 hrs
24hrs
48hrs
72hrs

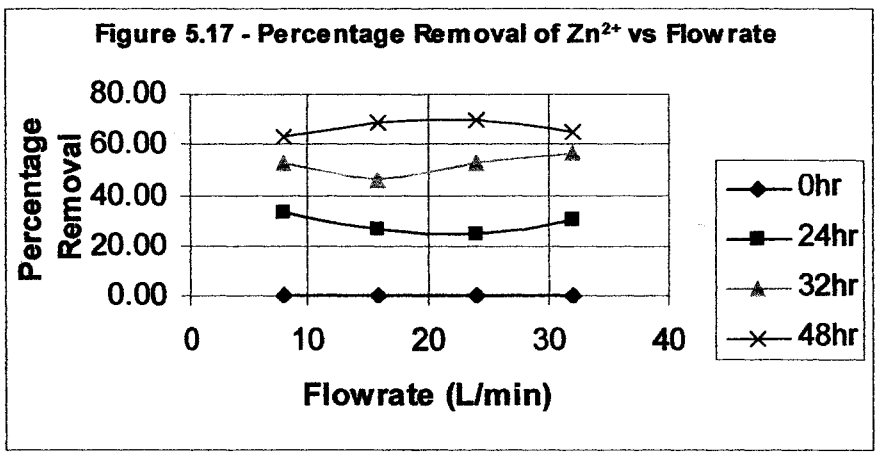
Figure 5.17 - Percentage Removal of Zn^{2+} vs Flowrate
Percentage Removal
80.00
60.00
40.00
20.00
0.00
0 10 20 30 40
Flowrate (L/min)
0hr
24hr
32hr
48hr

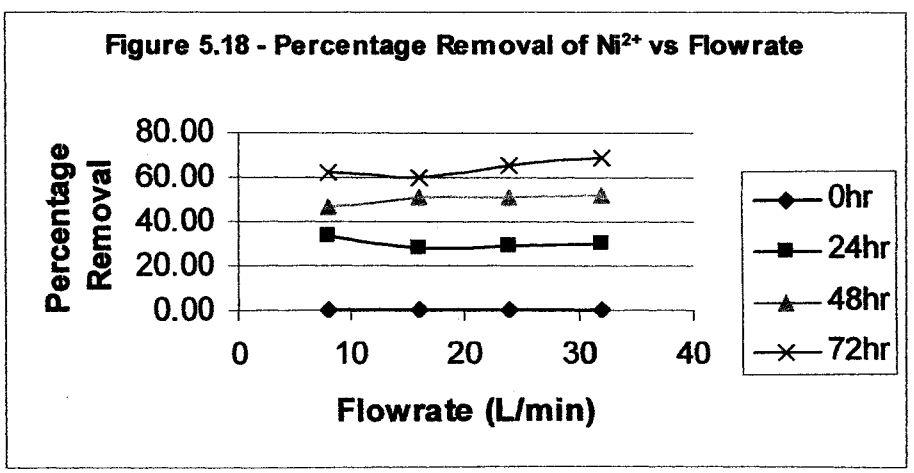
Figure 5.18 - Percentage Removal of Ni^{2+} vs Flowrate
Percentage Removal
80.00
60.00
40.00
20.00
0.00
0 10 20 30 40
Flowrate (L/min)
0hr
24hr
48hr
72hr

As shown in figures 5.16-5.18, for the range of liquid flowrate used in the present study, the liquid flowrate had no significant effect to the percentage removal of Methylene Blue, Zn^{2+} and Ni^{2+}. The main reason of the ineffectiveness of the flowrate to the Percentage Removal in the present study was due to the nature of the experimental setup. In the combined suspended photocatalytic operation, the dispersed titanium dioxide in water required constant mixing in order to prevent the titanium dioxide from settling to the bottom of the tank. Therefore, the effect of hydrodynamic change by the inlet flowrate may be overshadowed by the effect of vertical mixing due to the rotating paddles in the reactor. To demonstrate this in detail, the velocities of water flowing across the reactor, v_h, was rather small as shown in Table 5.13 below:

Table 5.13 – Linear velocity of liquid in the reactor

Flowrate (LPM)	Flowrate (m^3/min)	Velocity of liquid across the reactor, V_h (m/min)
8	0.008	0.0222
16	0.016	0.0444
24	0.024	0.0667
32	0.032	0.0889

On the other hand, the mixing paddle, as shown in the experimental setup, was rotating at 17 RPM. This is equivalent to a linear velocity, v_i, of 6.67m/min. At the highest flowrate, which is equivalent to velocity, v_h, of 0.089m/min, the vertical mixing, v_i, which is the mixing caused by the mixing paddle, is much higher than v_h. Whether the flowrate is 8LPM or 32LPM, v_h is much smaller than v_i. This indicated that the effect of the internal mixing, v_i, on the treatment of the wastewater was more significant than the effect of v_h. Therefore, the effect of hydrodynamic change by the inlet flowrate is relatively

insignificant compared to the effect of vertical mixing on the percentage removal of Methylene Blue, zinc and nickel ions.

5.7 The Effect of Wavelength on the removal of Methylene Blue, Zinc and Nickel ions by combined photocatalytic and electrochemical treatment

In order to facilitate a photocatalytic process which can be used to degrade pollutants in water, the role of the light is important. Theoretically, for titanium dioxide as a photocatalyst, the electron-hole can only be generated only if the wavelength is smaller than 380nm. In the present study, 3 UV lamps with wavelengths of 254, 302 and 365nm were tested using the same experimental setup for the treatment of Methylene Blue, Zn^{2+} and Ni^{2+}. The results obtained are plotted in figures (5.19-5.21)

Figure 5.19 - Percentage Removal of Methylene Blue vs Wavelength

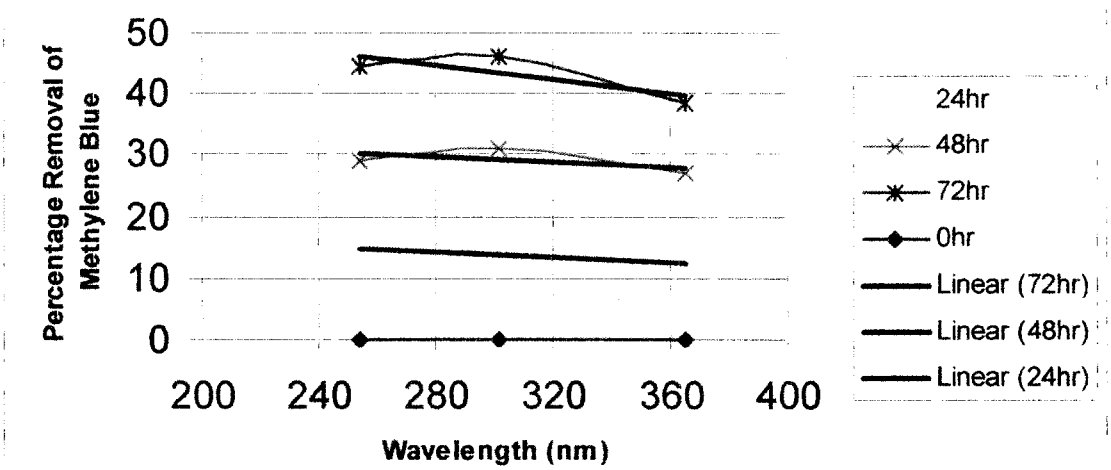

The percentage removal of Methylene Blue only decreased slightly at higher light wavelength. Further, all of the linear regression lines at 24, 48 and 72hours of treatment have negative slope. This suggests that the percentage removal of Methylene Blue isinversely related to the wavelength of the incident light. This can be explained by the inverse relationship between the wavelength and the energy, $hc/\lambda=E$. With higher energy, the probability for an electron to be promoted to the excited state is increased.

Figure 5.20 - Percentage Removal of Zn^{2+} vs Wavelength

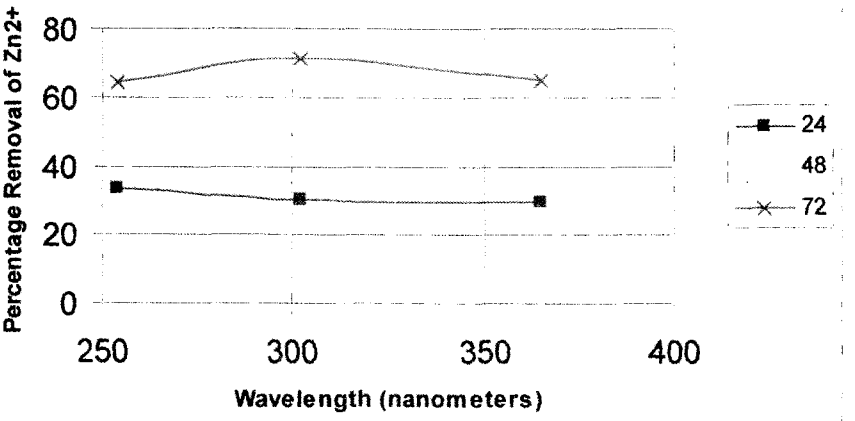

Figure 5.21 - Percentage Removal of Ni^{2+} vs Wavelength

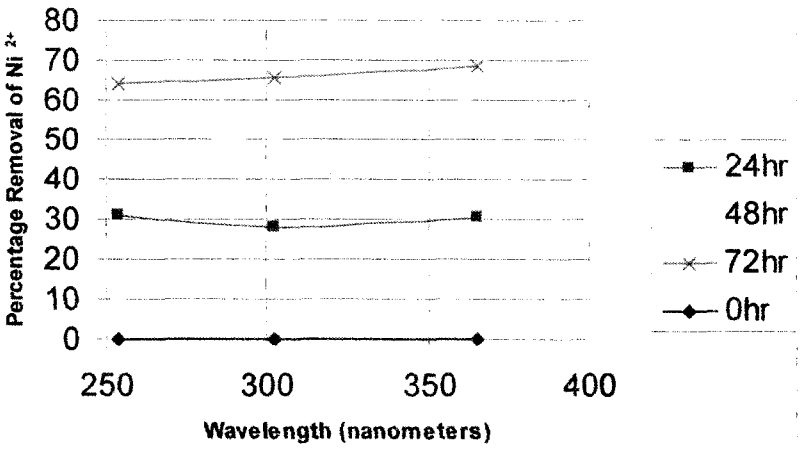

As shown in figure 5.20 and 5.21, UV wavelength had no significant effect on the percentage removal of Zn^{2+} and Ni^{2+}. This is in agreement with the observation given in the previous section that the heterogeneous photocatalysis is ineffective for the treatment of dissolved metals.

5.8 The Effect of pH on the treatment of Methylene Blue, Zinc and Nickel ions by combined photocatalytic and electrochemical method

To determine the effect of pH on the treatment of Methylene Blue by combined photocatalytic and electrochemical method, 3 different initial pH levels (2.1, 5.6, 10) were tested. The results obtained are plotted in Figure 5.22:

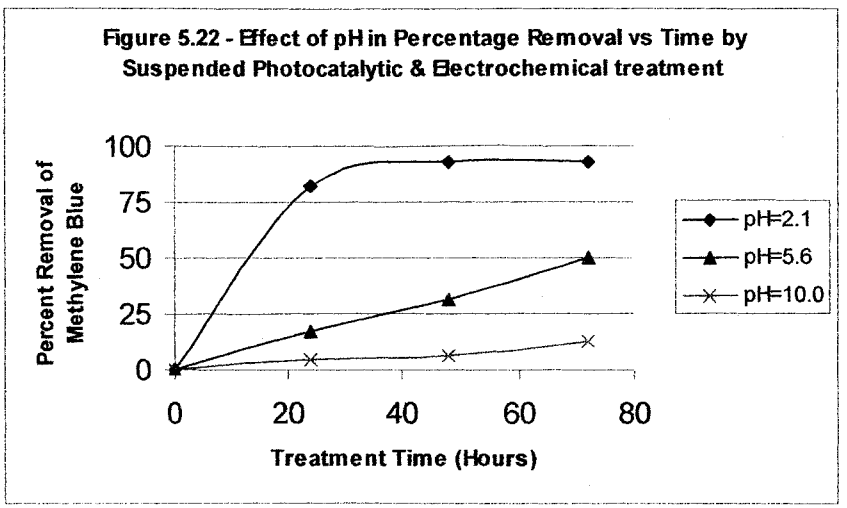

It appeared that the Percentage Removal of Methylene Blue increased when the pH was lowered. The pH dependent behavior can be explained by the effect of pH on both the semiconductor potential and the surface dissociation of the hydrated TiO_2. The Nerstian shift of the band edges to more negative values with increase in pH, leads to a decreasing oxidiation potential of h_{vb}^+ at high pH. Also, the change in photocatalytic activity may result from changes in pH. In water, the surface of a TiO_2 crystals is covered with TiOH in water:

$$TiOH \Leftrightarrow TiO^- + H^+ \qquad (5.15)$$

Since the dissociation does not proceed in acidic solutions, the photocatalytic activity is enhanced at lower pH (Chanda et al, 1998). Also, acidic condition at low pH caused anodic corrosion from the stainless steel anode generated iron ions, which might promote

the generation of hydroxyl radicals as mentioned previously. On the other hand, during the experimental trial with high pH (pH=10), it was observed that most of the zinc and nickel ions precipitated. These precipitated metals might block the incident light to reach for the photocatalyst.

CHAPTER 6 – CONCLUSIONS AND REMCOMMENDATIONS

6.1 Conclusions

From the results obtained in the present study, the following conclusions were drawn:

1. Suspended Photocatalytic treatment using suspended titanium dioxide as the Photocatalyst was effective for the removal of Methylene Blue at low concentration. Immobilized Photocatalytic treatment using titanium dioxide immobilized by PVC resin on a supporting material was effective for the removal of Methylene Blue at low concentration. The Removal of Methylene Blue by photocatalysis conformed to 1st order kinetics. The dissolved metals, Zn^{2+} and Ni^{2+}, however, did not exhibit change by photocatalytic treatment.
2. Methylene Blue, Ni^{2+} and Zn^{2+} at a low concentration were removed effectively using electrochemical deposition.
3. Methylene Blue could be degraded more efficiently by the combined Photocatlytic and Electrochemical process than by the photocatalytic oxidation or the electrochemical deposition alone. The percentage removal of Methylene Blue in combined Suspended Photocatalytic and Electrochemical process was 46.1% after 72 hours of treatment, while it was only 36.1% for the Suspended Photocatalytic process and 23.5% for the Electrochemical process. Similar observation was noted for the combined Immobilized Photocataltyic and Electrochemical process. The percentage removal of Methylene Blue in the combined Immobilized Photocatalytic and Electrochemical process was 28.9%, while it was only 14.9% for a single Immobilized Photocatalytic method and 23.5% for the single electrochemical method.

4. The flowrate had no significant effect on the percentage removal of Methylene Blue, Ni^{2+} and Zn^{2+}. This was due to the hydrodynamic effect caused by the internal mixing which was much higher than that of the change in flowrate.
5. A decrease of 8% Methylene Blue removal was observed when the wavelength was increased after 72hours of treatment. The dissolved metals did not have significant effect with different wavelengths.

6.2 Recommendations

From the observations obtained in the present study, the following recommendations were drawn:

1. Use higher light intensity Ultraviolet Lamps:

   One of the most important factors that caused the low kinetic rate constant, K, for the removal of Methylene Blue is the lack of light intensity. For all experiments performed, an average light intensity of $0.5mW/cm^2$ was recorded. Based on various reports such as those from Kuo & Ho and Rajeshwar et al, more than $1mW/cm^2$ was used for water volumes smaller than 10 liters (Kuo and Ho, 2001 and Rajeshwar et al, 1998). Therefore, more than $30mW/cm^2$ was recommended for future study with the present experimental unit (about 320L).

2. Use a well-established immobilization technique

   According to Rao *et al*, the effectiveness for the photocatalyitc treatment of water constituents in most commonly used immobilization method degrades after prolonged use (Rao et al, 2004). Although the immobilization method mentioned in the present study is relatively quick and simple, it was observed that the treatment efficiency slowly decrease to zero after prolonged use. Therefore, well established immobilization techniques or commercialized immobilization techniques, which are typically more stable after prolonged use, such as ARC-FLASH, are recommended.

3. Relocate the drain valve:

   Some sludge including titanium dioxide was leftover at the bottom of the reactor after each experiment. It was due to the improper location of the drain valve.

Therefore, it is recommended to change the location of the drain valve to the bottom center of the reactor to ensure complete removal of sludge after each experiment.

4. Investigate other process parameters:

   Further study should be carried out in order to investigate the relationship between the concentration of the organic matter, dissolved metals in the wastewater and the required voltage at which the organics might be involved in the electrode reactions. Also, the effect of the light intensity upon the removal of the organic should be investigated since the light intensity is directly related to the excitation of the electron-hole pairs, which lead to the oxidation of the organic matters. In addition, the rotational speed of the rotating disc in immobilized photocatalytic treatment on the removal of organics should be investigated since the hydrodynamic effect at the photocatalyst surface influences the mass transfer rate of the organics from the water to the photocatalyst surface (Dionysiou et al, 2002).

5. Immobilize titanium dioxide at the anode of the electrochemical cell

   According to Byrne et al, it is possible to immobilize titanium dioxide at the anode of an electrocell (Byrne et al, 1999). This allows an enhanced photocatalytic oxidation of organic matter at the anode due to the external current. At the same time, metal ions can be reduced at the cathode of the electrocell. It is believed that the removal of the organic may be increased compared to the present study as the supporting material, which is also the anode, was externally charged.

6. Possible study: Triple combination of electrochemical, biological and photocatalytic treatment

According to Anderson et al, photocatalytic treatment is capable of increasing the biodegradability for some types of compound (Anderson et al, 1997). For example, according to the results of a report by Lam et al, wastewater generated from the electro-coating industry is typically contained dissolved metals and PGME, propylene glycol methyl ether. Since the PGME is not 100% biodegradable, it may be beneficial to investigate a triple combination of biological, photocaltytic and electrochemical degradation of the organic and heavy metals in wastewater (Lam, 2002)

Reference

An C, Zhu H, Xiong Y. "Feasibility study of photoelectrochemical degradation of methylene blue with three-dimensional electrode-photocatalytic reactor" Chemosphere, Vol. 46, pp. 897–903 , 2002.

An C, Xiong Y, Li G, Zha C, Zhu X. "Synergetic effect in degradation of formic acid using a new photoelectrochemical reactor." Journal of Photochemistry and Photobiology A: Chemistry, Vol. 152 pp. 155–165, 2002.

Anderson W; Bolduc L. "Enhancement of the biodegradability of model wastewater containing recalcitrant or inhibitory chemical compounds by photocatalytic preoxidation" Biodegradation Vol. 8, pp. 237–249, 1997.

Atkins PW, Physical Chemistry. WH Freeman and Company, New York, 1986.

Boithi E. "Removal of Zinc and Nickel from Effluent Waters of an electroplating plant using a batch reactor" Ryerson University, 2002.

Byrne J.A., Eggins B.R., Byers W, Brown N.M.D. "Photoelectrochemical cell for the combined photocatalytic oxidation of organic pollutants and the recovery of metals from waste waters" Applied Catalysis B: Environmental, Vol. 20, pp. 85-89, 1999.

Callister, W. Materials Science and Engineering An Introduction. 5th Edition. John Wiley & Sons, Inc. Toronto, 1999.

Chanda M, Naskar SS, Pillay A. "Photocatalytic degradation of organic dyes in aqueous solutions with TiO2 nanoparticles immobilized on foamed polyethylene sheet" Journal of Photochemistry and Photobiology A: Chemistry, Vol. 113 pp. 257-264, 1998.

Chen D, Ray A.K. "Removal of toxic metal ions from wastewater by semiconductor Photocatalysis" Chemical Engineering Science, Vol. 56 , pp. 1561-1570, 2001.

Doan H.D., Wu J, Boithi E, Storrar M. "Treatment of wastewater using a combined biological and electrochemical technique" Journal of Chemical Technology and Biotechnology, Vol. 78, pp. 632-641, 2003.

Dionysiou D.D. ,Makram T, Baudin I, Laliné J.M. "Oxidation of organic contaminants in a rotating disk photocatalytic reactor: reaction kinetics in the liquid phase and the role of mass transfer based on the dimensionless Damköhler number"Applied Catalysis B: Environmental, Vol. 38, pp.1–16, 2002.

Dionysiou D.D., Balasubramanian G, Suidan M.T., Khodadoust A.P., Baudin I and Laine J-M. "Rotating Disk Photocatalytic Reactor: development, characterization, and evaluation for the destruction of organic pollutants in water" Wat. Res. Vol. 34, No. 11, pp. 2927-2940, 2000.

Drinan, J E. Water & wastewater treatment: A guide for the nonengineering professional. Technomic publishing company, Inc, Pennsylvania pp. 133-137;159-199, 2001.

Dziewinski J, Marczak S, Nuttall E, Purdy G, Smith W, Taylor J and Zhou C, "Developing and testing electrochemical methods for treating metal salts, cyanides and organic com-pounds in waste streams." Waste Management, Vol. **18** pp. 257–263, 1998.

F. Goodridge, K. Scott Electrochemical Process Engineering A Guide to the Design of Electrolytic Plant. Plenum Press, New York, 1995.

Fujishima, A, Hashimoto, K, Watanabe, T. TiO_2 Photocatalysis Fundamentals and Applications. Bkc Inc., Tokyo, 1999.

Gulyas H, "Processes for the removal of recalcitrant organics from industrial wastewaters." Wat Sci Tech, Vol. 36(2–3) pp. 9–16, 1997.

Guillard C, Lachheb H, Houas A, Ksibi M, Elaloui E, Herrmann J-M. "Influence of chemical structure of dyes, of pH and of inorganic salts on their photocatalytic degradation by TiO2 comparison of the efficiency of powder and supported TiO_2" Journal of Photochemistry and Photobiology A: Chemistry, Vol. 158, pp. 27–36, 2003.

Hartmut Wendt, G. Kreysa. Electrochemical Engineering Science and Technology in Chemical and Other Industries. Springer-Verlag Berlin Heidelberg, New York, 1999.

Houas, A, Lachheb, H, Ksibi, M, Elaloui, E, Guillard, C, Herrmann, J-M. "Photocatalytic degradation pathway of methylene blue in water." Applied Catalysis B: Environmental Volume 31 pp.145-157, 2001.

J.S. Newman. Electrochemical Systems. 2nd Edition. Prentice-Hall Canada Inc., Toronto. 1991.

Janssen, F.J.J.G., Van Santen, R.A. Environmental Catalysis Catalytic Science Series - volume.1 Imperial College Press, 1999.

K. Vinodgopal, P.V. Kamat. "Electrochemically assisted photocatalysis using nanocrystalline semiconductor thin films" Solar Energy Materials and Solar Cells, Vol. 38 pp. 401-410, 1995.

Kaneko, M. Okura, I. Photocatalysis Science and Technology. Springer-Verlag Berlin Heidelberg, New York, 2002.

Kuo, W; Ho P. "Solar photocatalytic decolorization of methylene blue in water" Chemosphere 45 pp. 77-83, 2001.

Kwon C.H., Shin H, Kim J.H., Choi W.S., Yoon K.H. "Degradation of methylene blue via photocatalysis of titanium dioxide" Materials Chemistry and Physics, Vol. 86, pp78–82, 2004.

Lakeshmi, S. Renganathan, R. Fujita, S. "Study on TiO2-mediated photocatalytic degradation of methylene blue" Journal of Photochemistry and Photobiology A: Chemistry Volume 88 pp.163-167, 1995.

Lam C, "Optimum Aeration Interval for BOD Removal using a Packed Column Under a Cyclic Operation" Ryerson University, 2002.

Mrowetz, M; Selli, E. "Effects of iron species in the photocatalytic degradation of an azo dye in TiO_2 aqueous suspensions" Journal of Photochemistry and Photobiology A: Chemistry, Vol. 162 pp.89–95, 2004.

Malato, S; Dibier R. "Solar photocatalysis: A clean process for water detoxification" The Science of the Total Environment, Volume 291, pp.85-97, 2002.

Metcalf & Eddy Wastewater Engineering Treatment and Reuse. 4th Edition. McGrawHill Toronto, 2003.

Pelegrini R, Peralta-Zamora P, Andrade AR, Reyes J, Durán N. "Electrochemically assisted photocatalytic degradation of reactive dyes." Applied Catalysis B: Environmental, Vol. 22, pp. 83–90, 1999.

Pelizzetti, E, Serpone, N. Photocatalysis Fundamentals And Applications. John Wiley & Sons, Toronto, 1989.

Pozzo R.L., Baltanas M.A., Cassano A.E. "Supported titanium dioxide as photocatalyst in water decontamination: State of the Art" Catalyst Today, Vol. 39, pp. 219-231, 1997.

Rajeshwar K, Ibanez J. Environmental Electrochemistry Fundamentals and Applications in Pollution Abatement. Academic Press, Toronto, 1997.

Rajeshwar, K; Sopajaree, K; Qasim A; Basak S. "An integrated flow reactor-membrane filtration system for heterogeneous photocatalysis. Part I: Experiments and modeling of a batch-recirculated photoreactor" Journal of Applied Electrochemistry 29: pp533-539, 1999.

Rao K.V.S., Subrahmanyam M, Boule P. "Immobilized TiO2 photocatalyst during long-term use:decrease of its activity" Applied Catalysis B: Environmental, Vol. 49, pp239–249 ,2004.

Raub E., Muller, K. Fundamentals of Metal Deposition. Elsevier publishing company, New York, 1967.

Roventi G, Fratesi R, Della Guardia RA and Barucca G, "Normal and anomalous codeposition of Zn–Ni alloys from chloride bath." J Appl Electrochem, Vol. 30, pp. 173–179, 2000.

Schiavello, M. Photocatalysis and Environment Trends and Applications. Kluwer Academic Publishers, London, 1987

Schiavello, M. Heterogenous Photocatalysis. John Wiley & Sons, Toronto. 1997

Sheffield Hallam University
http://www.shu.ac.uk/schools/sci/chem/tutorials/molspec/beers1.htm

Storrar M. "Electrochemical and Biological Treatment of wastewater from the automotive industry." Ryerson University, 2002

Skelton, R.L. Fabiyi, M.E. "Photocatalytic mineralisation of methylene blue using buoyant TiO2-coated polystyrene beads" Journal of Photochemistry and Photobiology A: Chemistry, Vol. 132, pp. 121–128, 2000.

Skoog, D; Holler, F; Nieman, T. Principles Of Instrumental Analysis. 5th Edition Saunders College Publishers, Toronto. 1998.

Vlyssides AG, Papaioannou D, Loizidoy M, Karlis PK and Zorpas AA. "Testing an electrochemical method for treatment of textile dye wastewater." Waste Management , Vol. 20, pp. 569–574, 2000.

Zumdahl, S. Chemical Principles 2nd Edition. D. C. Heath and Company, Toronto. 1995.

Arc-Flash http://www.arc-flash.co.jp/arc/e/02f.html

Appendix A - Error Analysis

There are some experimental uncertainties associated with the results as listed below:

1. Absorbance measurement interference by suspended titanium dioxide:

   In experimental trials involving suspended photocatalytic treatment, the samples collected were allowed to settle for 24 hours before the clear liquid was taken for absorbance measurement. However, during transfer of samples some titanium dioxide might have remixed with the water sample. This may cause some positive error in absorbance reading. Nevertheless, this was a systematic error and cancelled out in comparison among the runs.

2. Titanium dioxide holdup at the storage tank:

   In experimental trials involving suspended photocatalytic treatment, due to the simple structure of the storage tank, significant amount of titanium dioxide were left in the storage tank after 72 hours operation. The amount of this holdup of titanium dioxide seemed to be directly related to the flowrate used in the experiment. If this holdup of titanium dioxide were not present, the efficiency of the photocatalysis reported could have been higher.

3. Water evaporation during the experiment:

   For each experimental run, the final concentration was probably lower than the reported value, i.e. the percentage removal was higher, as some water evaporated during the experiment and the amount of water that was electrolyzed was not known.

Appendix B – Sample Calculations

Sample Calculation for the determination of percentage removal of Methylene Blue:

From Appendix A – Experimental data of Trial 1:

Methylene Blue content by absorbance

Time	Absorb	%	% Rem
0	0.681	100	0
24	0.587	86.20	13.80

The percentage absorbance at 24 hours is:

$$\frac{\text{Absorbance @ time 0}}{\text{Absorbance @ time t}} \times 100\% = \frac{0.587}{0.681} \times 100\% = 86.20\%$$

The percentage removal of Methylene Blue at time t
= Percentage absorbance @ 0 hour – Percentage absorbance @ time t

100-86.20=13.80

Sample Calculation for the determination of percentage removal of Zinc ion, Zn^{2+}:

Zinc content by test #27

Time	Reading	Concentration (mg/L)	%	% Rem
0	3.2	48	100	0
24	2.36	35.4	73.75	26.25

Concentration (mg/L) @ 0hr = Spectrophotometer Reading x dilution factor
=3.2 x 15 = 48mg/L

The percentage of zinc at 24 hours is:

$$\frac{\text{Zinc @ time 0}}{\text{Zinc @ time t}} \times 100\% = \frac{35.4}{48.0} \times 100\% = 73.75\%$$

The percentage removal of Zi^{2+} at time t
= Percentage of zinc @ 0 hour – Percentage of zinc @ time t

100-73.75=26.25%

Sample Calculation for the determination of percentage removal of Nickel ion, Ni^{2+}:

Nickel content by test #41

Time	Reading	Factor (=4)	%	% Rem
0	9.32	27.96	100	0
24	7.15	21.45	76.72	23.28

Ni^{2+} concentration (mg/L) @ 0hr = Spectrophotometer Reading x dilution factor
=9.32 x 4 = 27.96mg/L

The percentage of nickel at 24 hours is:

$$\frac{Ni^{2+} \text{ @ time 0}}{Ni^{2+} \text{ @ time t}} \times 100\% = \frac{21.45}{27.96} \times 100\% = 76.72\%$$

The percentage removal of Ni^{2+} at time t
= Percentage of nickel @ 0 hour – Percentage of nickel @ time t

100-76.72=23.28%

Sample Calculation for the determination of velocity of liquid across the reactor, V_h (m/min) in Table 5.13:

For a flowrate, Q_{pipe}, of 8 liters per minute:

$$8\text{LPM} = \frac{8\text{ L}}{\text{min}} \times \frac{1\text{ m}^3}{1000\text{ L}} = \frac{0.008\text{ m}^3}{\text{min}}$$

Mass balance

$Q_{pipe} = Q_{reactor}$
Q_{pipe} = velocity of liquid across the reactor x Cross-section area of the reactor
$Q_{pipe} = V_h \times As$

$$V_h = \frac{Q_{pipe}}{As} = \frac{0.008\text{ m}^3/\text{min}}{(0.6\text{m} \times 0.6\text{m})}$$
$$= 0.0222\text{ m/min}$$

Uncertainty analysis calculation

By using the method of uncertainty analysis, the uncertainty of the percentage removal of nickel ions can be calculated as follows:

$$\%Ni = \left(\frac{C_{initial} - C_{final}}{C_{initial}} \right) \times 100\% \tag{A1.1}$$

$$w_{\%Ni} = \left[w_1 \left(\frac{dw_{\%Ni}}{d\,c_{initial}} \right)^2 + w_2 \left(\frac{dw_{\%Ni}}{d\,c_{final}} \right)^2 \right]^{1/2} \tag{A1.2}$$

$$\frac{dw_{\%Ni}}{d\,c_{final}} = -\left(\frac{1}{c_{initial}} \right) \tag{A1.3}$$

$$\frac{dw_{\%Ni}}{d\,c_{initial}} = c_{final} \times ln[\,c_{initial}] \tag{A1.4}$$

From Table 5.4, $C_{initial}$ = 36.5mg/L, C_{final} =12.0mg/L, applying equation (A1.3-A1.4):

$$\frac{dw_{\%Ni}}{d\,c_{initial}} = 12.0 \times ln[36.5] = 43.168 \tag{A1.5}$$

$$\frac{dw_{\%Ni}}{d\,c_{final}} = -\left(\frac{1}{36.5} \right) = -0.0274 \tag{A1.6}$$

Based on information suggested by the supplier of the photometer, Orbeco-Hellige colorimeter (model 975-MP), the uncertainty values, w_1 and w_2 is:

$$w_1 = w_2 = 0.02 \tag{A1.7}$$

Substituting equation A1.5-A1.7 to A1.2 gives:

$$w_{\%M} = [0.02(43.168)^2 + 0.02(-0.0274)^2]^{1/2} = 6.1 \quad \text{(A1.8)}$$

Therefore, by using uncertainty analysis, the uncertainty of the percentage removal of nickel is found to be 6.1%. In section 5.5, after 72 hours of treatment, the percentage removal of nickel is 67.0 ± 6.1 %.

Similarly, by using uncertainty analysis, the uncertainty of the percentage removal of zinc is found to be 9.1%. In section 5.5, after 72 hours of treatment, the percentage removal of zinc is 63.4 ± 9.1 %.

Appendix C – Determination of the absorption peak for Methylene Blue

Date: 4/21/4 Time: 12:21:25 PM

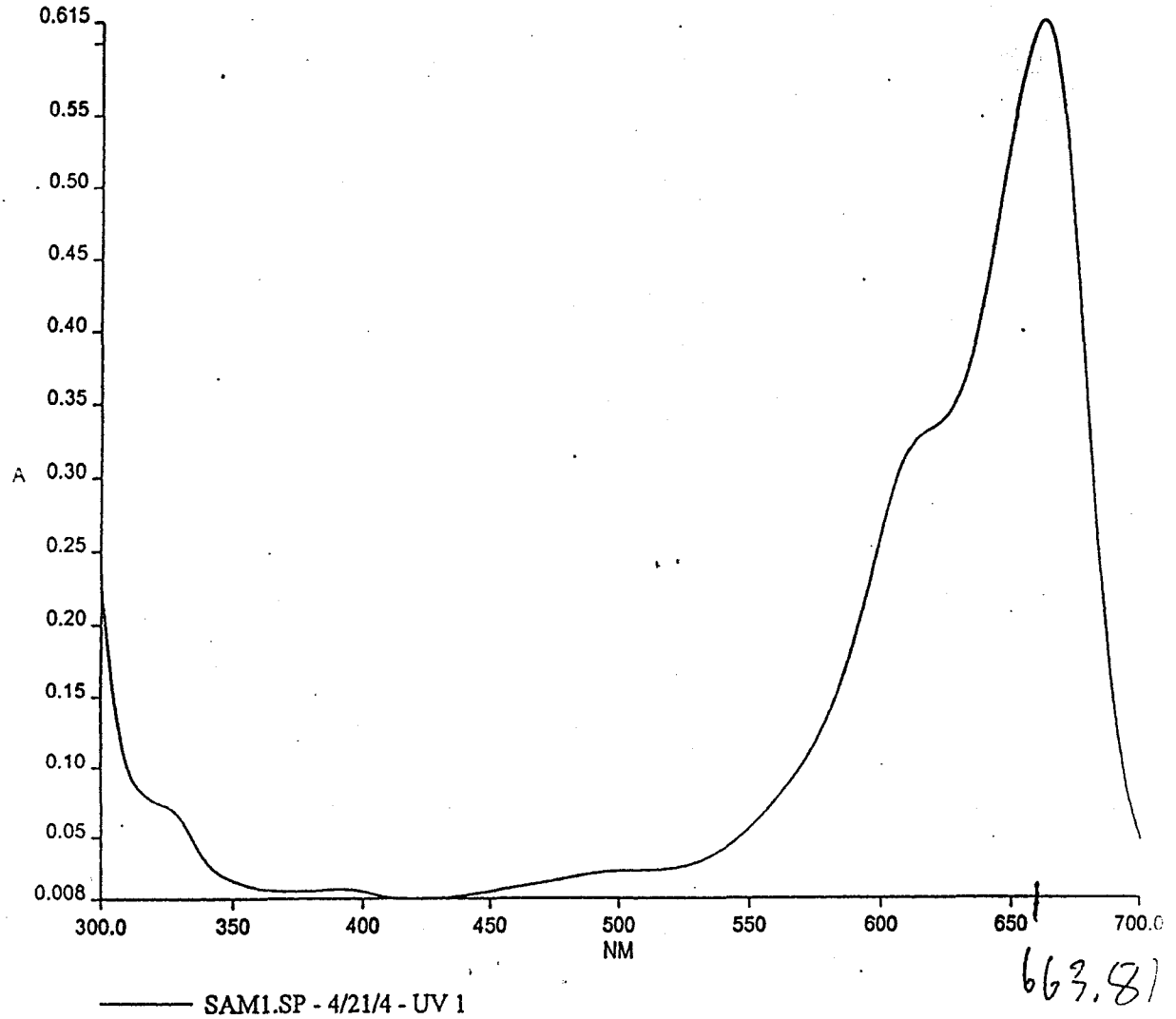

A = Absorbance
NM = Wavelength in nanometers

NICKEL (NICKEL)
975-MP Test No. 41
Filter Wavelength: 528
Range: 0-12 mg/L and higher
Method: Dimethylgloxime (Heptoxime)

NICKEL "Quick'n'Easy" TEST KIT No. 975-41 includes:
2 oz. No. R-3947 Ammonium Citrate Solution., with 1 mL pipet (Code B,5)*
1 oz. No. R-3956 Iodine Solution, with 0.5 mL pipet (Hazard Code B,5)*
4 oz. No. R-386 Ammonium Hydroxide 1:1, with 1 mL pipet (Code A,2)*
1 oz. No. R-2019 Dimethylglyoxime, 1% Alcholic, in metered dropper bottle (Hazard Code B,5)*

BEFORE STARTING: Read General Instructions, safety precautions and Notes. Do not intermix glass and plastic Tubes.

1. **PREPARATION OF "BLANK TUBE"**

   a. Fill a clean, dry tube to 10 mL mark with sample. Cap and set aside for use in Step 3.

2. **PREPARATION OF "SAMPLE TUBE"**

   a. Fill another clean, dry tube to 10 mL mark with sample.

   b. Add 2 mL R-3947 Ammonium Citrate Solution using pipet in bottle twice. Cap tube and invert several times to mix.

   c. Remove cap, add 1.0 mL R-3956 Iodine Solution using pipet in bottle twice. Cap tube and invert several times to mix.

   d. Remove cap, add 4 mL R-386 Ammonium Hydroxide 1:1 using the 1 mL dropper bottle 4 times. Cap tube, mix as before.

   e. Add 18 drops of R-2019 Dimethylglyoxime Reagent. Replace cap and while holding cap securely, invert several times. Note time, allow 7 minutes for color development.

3. **Follow OPERATING INSTRUCTIONS** to obtain test results in terms of mg/L (ppm) Nickel (Ni).

NOTE 1: The Ammonium Citrate eliminates Iron and Aluminum interference. Copper does not interfere up to 3 mg/L.

NOTE 2: If screen reads **"Dilute & Retest"** or to confirm a reading at or near 12 mg/L, dilute a fresh sample with distilled or deionized water, retest, and multiply the result by the dilution factor as explained in Section 2.4

*For Reagent Hazard Code explanations, see Section 6.

* * * * *

ZINC (ZIN
975-MP Test No. 7
Filter Wavelength: 6
Range: 0-4.0 mg/L Zn and high
Method: Zinc

ZINC "Quick'n'Easy" TEST KIT No. 975-27 contains:
1 Pkg of 50 RT-112 Zinc Tablets (Hazard Code: 0,5)*
1 ea. 432-SRP Tablet Crusher/Stirring Rod

BEFORE STARTING: Read General Instructions, safety precautions and Notes. Do not intermix glass and plastic Tubes.

SAMPLING AND STORAGE: Collect samples in plastic bottles that have been was with 1:1 Hydrochloric Acid (R-405) and thoroughly rinsed with Deionized Water (R-3684). Samples can be stored at least six months at room temperatur if adjusted to pH 2 (use about 2 mL nitric acid per liter). Before testin adjust sample to pH 4 - 5 with 1.0 N Sodium Hydroxide (R-538), but do not exceed pH 5, to avoid loss of zinc as a precipitate.

1. **PREPARATION OF "BLANK TUBE":**

   a. Fill a clean, dry tube to the 10 mL mark with sample. Cap and set it aside for Step 3.

2. **PREPARATION OF "SAMPLE TUBE":**

   a. Fill another clean, dry tube to the 10 mL mark with sample. (If samp has high chlorine residual, add one No. RT-113 Zinc-Dechlorinating tablet, crush, cap tube and mix to dissolve).

   b. Add one Zinc tablet, crush, cap, and mix to dissolve. Note the time.

   c. Allow sample to stand for five minutes, then mix again to assure com dissolution of tablet material.

3. **Follow OPERATING INSTRUCTIONS** to obtain test result in terms of mg/L (p Zinc.

NOTE 1: If screen reads **"Dilute & Retest"** dilute a fresh sample with disti or deionized water, retest, and multiply the result by the dilution factor explained in Section 2.4.

NOTE 2: Copper also produces color with this reagent (RT-112). If the pr of copper is suspected redo the test (after reading Zinc result in Step 3 using Blank Tube from Step 1a and Sample Tube from Step 2c. Add one EDTA Tablet No. RT-114 to Sample Tube, crush, cap and mix to dissolve. Follow Operating Instructions to obtain results in terms of mg/L Copper (disregua screen name of "Zinc"). This copper reading must be subtracted from the initial Zinc reading to give the corrected Zinc result.

Continue

degussa.

Aerosil & Silanes

Product Information

Titanium Dioxide P 25

Hydrophilic fumed Titanium Dioxide

Titanium Dioxide P 25 is a highly dispersed titanium dioxide manufactured according to the AEROSIL® – process.

Applications and Properties

Applications

- Catalyst carrier
- Active component for photocatalytic reactions
- Heat stabilizer for silicone rubber

Properties

- Process related high purity
- Heat stabilizing properties for silicone – elastomers through its effect on redox reactions

  Thereby:
  - Improvement of ageing properties at high temperature (≥ 200°C)
  - Positive impact on flammability protection

Physico–chemical Data

Properties	Unit	Typical Value
Specific surface area (BET)	m^2/g	50 ± 15
Average primary particle size	nm	21
Tapped densitiy (approx. value) * *acc. to DIN ISO 787/XI. Aug. 1983*	g/l	130
Moisture * *2 hours at 105 °C*	%	≤ 1.5
Ignition loss *2 hours at 1000 °C based on material dried for 2hours at 105 °C*	%	≤ 2.0
pH-value *in 4% Dispersion*		3.5 – 4.5
TiO_2-content (1) *(1) based on ignited material*	%	≥ 99.50
Al_2O_3- content (1)	%	≤ 0.300
SiO_2- content (1)	%	≤ 0.200
Fe_2O_3- content (1)	%	≤ 0.010
HCL- content (1)		≤ 0.300
Sieve residue by Mocker, 45 µm *acc. to DIN ISO 787/XVIII, Apr. 1984*	%	≤ 0.050

* ex plant

The data represents typical values and not production parameters.